EPA-R2-73-207

January 1973

Environmental Protection Technology Series

Development of Improved Systems for Obtaining Time Integrated Measurements of SO_2, NO_2, NO_x, and Other Pollutants

Office of Research and Monitoring
U.S. Environmental Protection Agency
Washington, D.C. 20460

EPA-R2-73-207

Development of Improved Systems for Obtaining Time Integrated Measurements of SO_2, NO_2, NO_x, and Other Pollutants

by

Victor R. Huebner

Instra-Tech, Inc.
1223 South State College Boulevard
Fullerton, California 92631

Contract No. 68-02-0318
Program Element No. 1A1010

EPA Project Officer: Andrew E. O'Keeffe

Chemistry and Physics Laboratory
National Environmental Research Center
Research Triangle Park, North Carolina 27711

Prepared for

OFFICE OF RESEARCH AND MONITORING
U. S. ENVIRONMENTAL PROTECTION AGENCY
WASHINGTON, D.C. 20460

January 1973

This report has been reviewed by the Environmental Protection Agency and approved for publication. Approval does not signify that the contents necessarily reflect the views and policies of the Agency, nor does mention of trade names or commercial products constitute endorsement or recommendation for use.

TABLE OF CONTENTS

LIST OF TABLES

LIST OF FIGURES

1. Introduction and Summary

This program was primarily directed toward investigating new and improved methods of detecting and recording the weak light emission resulting from the chemiluminescent reaction of air pollutants with specific gaseous reactants. Major emphasis was placed on attempting to use photographic film as both a detector and integrator for the light emission. The intent was to expose film to the chemiluminescent reaction, develop the film, and relate film density to accumulated air pollutant. The major problem was that it requires almost a million times as much light to produce a detectable response on a one inch square film plate as is required for a photomultiplier tube. This disadvantage can be minimized by concentrating the reaction over a very small surface area. Consequently reaction chambers having extremely small frontal areas were developed. Chambers that were .5mm diameter provided 1400 times as much light intensity. Unfortunately, this still wasn't enough to overcome photographic film's poor sensitivity.

Although the photographic film approach was unsuccessful, several avenues were explored that may be of value in the future. One of the more important findings was that the chemiluminescence reaction is primarily limited by physical mixing efficiency of the reactants. Long, narrow reaction chambers provided much better mixing efficiency. With excessively narrow tubes, however, optical reflectance losses counteracted any improved mixing efficiency. Nevertheless, moderately small diameter reaction chambers should yield better signals and make it possible to use small diameter detectors. The other major finding of interest was that permeation tubes could be effectively used to

meter in the reactant gas. This may make it possible to eliminate the need for auxiliary reactant gas cylinders.

Photon counting was then explored as a means of increasing the reliability and reducing the cost of chemiluminescent detectors. This approach was quite successful. A system was developed that amplified each photoelectron, discriminated against noise pulses, accumulated all the photon counts, and displayed the sum of the photon counts on a 5 x 7 light emitting diode display. The photon counting system was packaged in a housing and was shipped to EPA laboratories for further tests.

2. Overall objectives

Chemiluminescence techniques for monitoring air pollutants such as SO2, NO2, NOx, ozone, etc. are extremely sensitive and reliable. Their major advantage is that they require minimal mechanical components, and no wet chemicals. Although chemiluminescence methods are basically simple and reliable, they impose severe sensitivity requirements upon the optical detector system required to monitor light emission. Photomultiplier tubes coupled to high impedance analog amplifiers are utilized almost exclusively in commercial chemiluminescence instruments. These instruments generally perform quite well under controlled laboratory conditions where the temperature is held constant and technicians are available to zero and calibrate the instruments. One of the purposes of this program was to develop methods of detecting light emitted by chemiluminescence which are more stable and reliable than those presently used. The other prime objective of this program was to develop a simplified method of time-integrating and recording

the outputs of chemiluminescence instruments. Data reduction through time integration is a practical necessity for any large scale monitoring program. For time integration to be effective, instrument stability must be extremely good.

Present instruments must either have periodic manual calibration or have very expensive self-correcting circuitry if long term stability is required. Photomultiplier tube gain changes caused by temperature variations or power supply changes are excessively high. Even the best amplifiers are somewhat marginal in respect to zero drift for this application. Consequently primary effort was placed on elimination of the PMT system by utilizing photographic film as the detector as well as recorder. When this approach proved to be unsuccessful, digital photon counting methods were explored.

3. Basic Experimental Approach

3.1 General background

This program was oriented primarily towards the "readout" portion of air pollution monitors rather than towards the chemical transducer components. Consequently, a commercial ozone analyzer, the Meloy Laboratories, Inc. OA320, was purchased for this program. This analyzer is typical of the current state-of-the-art in pollution analyzers based on the chemiluminescence principle.

3.2 Specific Characteristics of the Meloy Analyzer

The Meloy ozone analyzer has a 19mm diameter by approximately 20mm deep chamber with concentric 6.3 and 3.2mmO.D. tubes terminating at the front glass wall to carry ethylene and air, respectively. This is essentially identical to the Nederbragt design. Recommended

flow rates are 1 liter per minute for air and 28ml/min. for ethylene. A UV lamp is used to provide ozone for calibration purposes, and gave a reading of 0.22ppm ozone under normal operating conditions.

When a Kodak Wratten 2B filter (400mm long pass) was inserted between the reaction chamber and the PMT, the ozone reading decreased from 0.22ppm to 0.14ppm. When a Wratten 12 filter (510nm long pass) was used, the ozone reading decreased to 0.02ppm. These results indicated that 36% of the light emission is below 400nm, 55% is between 400nm and 510nm, and only 9% of the light emission is greater than 510nm. These results agree with those of Hodgeson, et al[1].

In another series of tests, masks with various size center holes were placed over the reaction chamber. These results are shown in table 1. The data indicate that light emission probably is evenly

TABLE 1

Relative Light Emission from the Meloy Reaction Chamber

Diameter hole in mask	Hole Area	PMT Reading	Intensity/mm^2
6.0mm	28mm^2	.01ppm	3.6
10.5	86	.08	9.1
13.5	145	.14	9.7
19 (no mask)	284	.22	7.7

distributed throughout the reaction cell. The lower value for the smallest hole probably is due to a lower volume of gas since this space is occupied by the inlet tubes. The decline for the largest area probably is due to a restricted angle of view because of the chamber walls. Thus, it appears that light is emanating uniformly

1. Hodgeson, J.A., Martin, B.E., and Baumgardner, R. E. Laboratory Evaluation of Alternate Chemiluminescent Approaches for the Detection of Atmospheric Ozone. ACS Meeting, Chicago, Sept. 1970.

from all portions of the chamber. This would be the case if incomplete or just barely complete mixing of the ethylene and oxygen were occurring.

The response of the entire system was found to be $9x10^{-9}$ amperes per ppm ozone. If we assume reasonable values for typical PMT's, this corresponds to approximately $1x10^{-10}$ lumens, or $4x10^{-11}$ lumens per centimeter. As will be shown in table 2 this is about 100 fold less than the sensitivity threshold level for photographic film. The response was inversely proportional to air flow rate (when the ozone generator was used), and was moderately sensitive to ethylene flow rate. As will be seen later, this is symptomatic of incomplete reaction between ozone and ethylene.

3.3 Secondary standards

Several types of secondary light sources were used instead of the Meloy Chemiluminescence monitor in order to provide greater versatility and convenience. A Monsanto MV-1 light emitting diode (LED) was used in most cases. By appropriately adjusting the voltage and current-limiting resistors, highly reproducible light levels could be easily achieved. The LED light output was calibrated by measuring its output with the Meloy analyzer PMT, and recording the output in "equivalent parts-per-million ozone". In this manner, the relative sensitivity of experimental detection modes could be easily determined. The primary disadvantage of the LED standard was that light emission occurred at 610nm rather than at the 430nm peak wavelength of the ozone chemiluminescent reaction.

The other secondary standard consisted of a 24v. tungsten

filament lamp driven by a 24vdc power supply through a series of current limiting resistors. This lamp was optically coupled to the detector under test (or to the Meloy PMT for calibration) through a 60 mm long by 6.3 mm D. quartz fiber optic tube, a Schott BG 18 infra-red filter, and a Kodak Wratten 36 filter. This combination produced light with maximum intensity at 420nm. and a half-band width of 45nm. Although the tungsten lamp's output is less controllable than a LED's, it's better spectral properties was needed for some tests. In all cases, light output was cross-correlated with the response of the Meloy PMT system (indicated in ppm ozone), so that meaningful comparisons could be made.

4. Direct Photographic Film Detection

4.1 Basic Problems

Photographic film was utilized in an attempt to eliminate the present photomultiplier tube detection system because it has a long history of usage in low light level application. Photographic film also appeared to be highly advantageous for its simplicity in integrating and recording the relative light intensity. Unfortunately, photographic film also has two major disadvantages - reciprocity failure and a dependance upon light intensity rather than total quantity of light. Photographic film has a sensitivity threshold below which an image will not be formed regardless of exposure time. Consequently, low light levels will either have a very non-linear relationship to film density or will go undetected. The mode of sensitizing - through light intensity rather than light quantity further compounds this problem. Whereas PMT detectors linearly respond to total light

with no regard for light distribution, film response is based upon a light intensity per unit area relationship. The only feasible method of improving this situation is to concentrate the available light of reaction into a smaller area. However, since the chemiluminescence reaction is a gaseous reaction, the mixing problem becomes more severe as reaction tube area is decreased.

4.2 Basic Film Sensitivity Considerations[1]

Essentially all film manufactured today is based on the silver bromide reaction to light. The primary factor affecting film sensitivity is the concentration of sulfide specks at the surface of the silver crystals. These specks originate from high molecular weight compounds in the gelatin used as the film base (synthetic sulfur compounds give poor sensitization) and congregate at imperfections in the silver bromide lattice. These sulfide specks require a significant number of photon-generated electrons before they are capable of promoting silver bromide sensitization through an electron transfer process. This requirement for high concentrations of photon-generated electrons arises because of a competing electron capture process within the sulfide specks. Once this threshold level has been reached, the silver bromide conversion can proceed at a rate governed by light intensity. Larger silver bromide crystals hold more sulfide specks and absorb more light than smaller crystals, thereby having better sensitivity.

Sensitivity characterists of photographic film can be described by a density vs. light exposure curve similar to the one shown in

1. Extracted from "Photographic Film" by P. Glatkides, Fountain Press, London, 1958.

figure 1. All film exhibits a nominal density called "fog" with no light exposure. As the light is increased, the density begins increasing at the threshold point. The curve then assumes a curved toe, a linear section, and a curved shoulder. Very high light intensities create a density decrease called "solarization". Various systems are used to designate film speed. Perhaps the poorest system is the ASA system, which has no scientific basis, is only valid for high light levels, and cannot be determined with any reasonable degree of precision. For our purposes, the threshold level is of paramount importance and references to "sensitivity improvement" will refer to a decrease in the quantity of light required to reach the threshold level. Consequently, many of the observations made may appear to be contradictory to popularly accepted notions.

It is generally believed that film sensitivity can be improved by different developing procedures. Unfortunately, high speed developing techniques only improve contrast - they have no effect on the film threshold level. Since the ASA ratings are based on contrast ratios, darkroom manipulations will improve the ASA value. They can't make an invisible latent image appear if the film threshold hasn't been reached.

The addition of sensitization chemicals to unexposed film can greatly enhance sensitivity to long wavelength (red) light. They cannot improve the basic film sensitivity at its maximum sensitivity wavelength (350nm.) Thus, they serve only to extend the wavelength response characteristics and can do nothing to improve film response to the ozone chemiluminescence reaction, which already occurs near the maximum wavelength sensitivity.

Figure 1

Typical response curve for photographic film

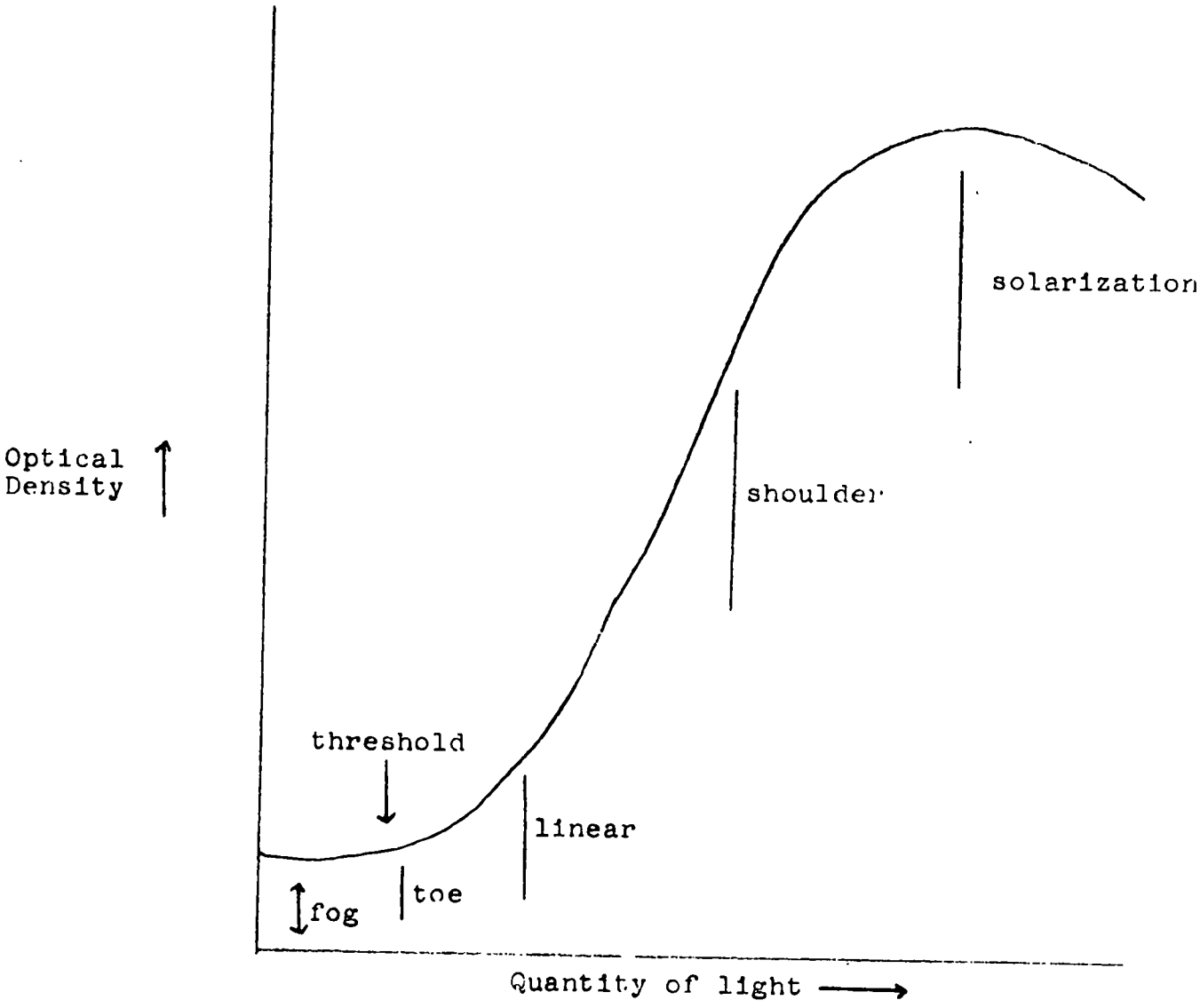

The most important sensitization techniques have consisted of pre- or post-exposure of the film to light, mercury vapor, ozone, sulfur dioxide, and various organic chemicals. These methods generally are optimized by exposing the film to a level just below its minimum threshold level, so that the image of interest can easily trigger the exposure. These methods require very careful control, and sensitization beyond a factor of 3 improvement generally is considered to be too tricky and unreliable.

4.3 Comparison of Different Films

Most of the faster types of film are compared in table 2. Column 1 lists the type of film, while its ASA value is listed in column 2. The third column lists the basic threshold of the film. These values, expressed in meter-candle-seconds, represent the lowest light level that gives a barely perceptible increase in density over normal film "fog". The threshold values were estimated in most cases from manufacturer's published curves. The next column lists the approximate ratios of sensitivity at 400 nm. versus that at 500 nm. This is important because film threshold values are determined at 500 nm, whereas the ozone chemiluminescense emission is near 400 nm. The columns listing the sensitivity ratios for longer exposure times ($s100sec/s1sec$, $s10^4sec/s100sec$.) reflect the increase in density with increased exposure time. Values of 100 would represent perfect linearity, while lower values are the result of reciprocity failure. The conversion to lumens per cm^2 puts film sensitivity on a radiometric basis. These values represent the lowest concentration of 400 nm. light that is capable of creating a film image.

Type IaO is an astronomy emulsion that is coated on glass slides.

It is characterized by a relatively slow speed but very little "reciprocity failure". Thus, for very long exposure times, it is more sensitive than some of the "fast" film. Tri-X is a high speed film that is widely used by photographers. It is more sensitive than IaO for exposure times less than 100 seconds, but its poor reciprocity characteristics make it less sensitive than IaO at longer exposure times. Royal Pan 4141 has approximately the same sensitivity as Tri-X. Polaroid 3000 film is definitely faster for exposure times less than 100 seconds, but has very poor time-integration properties with longer exposure times. Polascope 410 is not significantly better than Polaroid 3000 film.

In summary it can be concluded that Polaroid 3000 film is significantly more sensitive than IaO, but has approximately the same sensitivity as do the other films listed in table 1 if the exposure time is approximately 100 seconds. For very long exposure times, the excellent reciprocity characteristics of IaO make it superior to other films. However, since photomultiplier tubes typically have sensitivities of 1-5x 10^{-14} lumens per cm^2, even the best films have approximately 10,000 times poorer sensitivity than do photomultiplier tubes.

4.4 Laboratory tests of film sensitivity

In addition to a theoretical assessment of the film sensitivity problem, a large number of film tests were made using an MV-1 LED to simulate chemiluminescence. The standard procedure followed in all cases was to prepare the test set-up, attach the Meloy PMT and associated electronics, and then operate the LED at various current levels in order to obtain a plot of input current vs. "equivalent ppm ozone". In all cases, the LED current was less than one-tenth as great as the current required to be barely perceptible to a trained observer

TABLE 2

COMPARISON OF FILM SENSITIVITY

Film	ASA value	Threshold (s)	s400nm/ x500nm	s100sec/ s 1sec	s10^4sec/ s100sec	Lumen/CM^2 100sec	Lumen/CM^2 10^4sec
IaO	25	.01 meter candle seconds	1.0	100	70	1x10-8	1x10-10
Tri-X Pan	320	.001	1.0	15	5	7x10-9	1x10-9
Royal Pan 4141	400	.001	0.6	30	10	6x10-9	6x10-10
Polaroid 3000	3,000	.0003	1.0	10	2	3x10-9	1x10-9
Polascope 410	10,000	.0001	1.0	5	2	2x10-9	1x10-9

after 5 minutes of acclimation in a totally dark room. In other words, the light intensities were exceedingly low.

After the calibration curve for a particular test set-up had been prepared, the PMT was removed and photographic film was placed in the same relative orientation as the PMT cathode had been. Various current levels were than applied to the LED (one level for each film negative) until it was determined that no image had been recorded. The lowest current level applied to the LED that had resulted in an image (usually just barely perceptible) was then recorded as the minimum film threshold value. By referring to the current vs. equivalent ozone chart, this minimum threshold value could be reported in terms of equivalent ppm ozone".

The test procedure previously described was applied to Polaroid 3000 film. Results of these tests are shown in table 3. The exposure areas were estimated by measuring the developed negative's images. The LED current used is only of academic interest since the actual light reaching the film was greatly influenced by the test set-up. The

TABLE 3

Polaroid 3000 Sensitivity

LED test set-up	Exposure time	Exposure Area	LED Current	Equiv. Ozone	Ozone/ cm^2
One inch from film	1 min	3.0cm.^{2}	$7x10^{-5}$A	70ppm	23ppm
One inch from film	60	3.0	$3x10^{-5}$	30	10
Through 1.6mm x 45cm filter optic	5	.070	$1.6x10^{-5}$	2	28
Through 1.6mm x 30cm tube	3	.018	$5x10^{-5}$	.1	55
Through 0.8mm x 30cm tube	3	.005	$3x10^{-5}$	.04	80

equivalent ozone values were determined by comparing the LED current required to produce a barely perceptible image with the PMT output response for that current. The ozone per cm^2 values are simple arithmetic derivations based on exposure area and equivalent ozone threshold values.

The first test was made with the uncollimated LED one inch from the film. This resulted in a dense exposure in the center which diminished in intensity towards the edges. This non-uniformity would have a tendency towards lower equivalent ozone values. As may be seen, the 60 minute exposure only resulted in a factor of two sensitivity improvement over the one minute exposure time. This is the result of Polaroid film's poor reciprocity characteristics. When the LED light was transmitted through a fiber optic bundle, the total sensitivity was much enhanced (due to the smaller area over which the light was spread) but the sensitivity on a per unit area basis was approximately the same. Where a 1.6 mm or 0.8 mm teflon tube was used to transmit the light, their smaller exposure area created a better gross sensitivity value, but the sensitivity per unit area wasn't appreciably affected (within experimental error). It thereby appeared that Polaroid 3000 film has an apparent sensitivity threshold of between 23 and 80 ppm ozone when a one cm^2 area is utilized. This sensitivity is only improved by a factor of two when very long exposure times are used. This estimate is biased strongly in favor of the film, since the film sensitivity is essentially the same at 430 nm. (ozone chemiluminescence) or 610 nm. (LED), whereas the Meloy PMT has only 5% as much sensitivity to 610 nm. radiation as it does to 430 nm radiation. Thus, the true equivalent sensitivity of Polaroid film is in the neighborhood of 1000 ppm. ozone/cm^2.

Since PMT systems can easily detect 10ppb ozone, a one cm^2 Polaroid system is approximately 100,000 times less sensitive than a PMT. This value agrees quite well with the factor of 10,000 calculated for the best film in a theoretical system. Thus, the film system must overcome a 10,000 - 100,000 fold disadvantage before it can compete with a PMT system. One method, which is feasible only for astronomy emulsions such as Kodak Ia-0, is to integrate the available light over exceedingly long time intervals. This may provide up to a factor of 100 improvement under ideal conditions. The other technique is to reduce the frontal area of the reaction chamber so that the chemiluminescence is concentrated in a smaller area, thereby increasing the intensity per unit area. Simple gas dynamic considerations dictate that the optimal chamber configuration would be a long narrow tube with infinitely good internal reflectivity. These types of chambers will be discussed in section 4.5.

In order to accomodate the astronomy type film plates and to hold the long tubular types of reaction chambers that appeared to be needed, a special camera chamber was designed and built. This is shown in figure 2. The rubber gasket was sandwiched between the upper and lower halves to provide a light-tight, gas-tight seal. The lower chamber contains an aluminum film holder that can be positioned by means of a rod sealed by O-ring bushings. The upper section contains a light-emitting diode holder, a holder for chemiluminescence reaction chambers, and a vacuum line.

All initial tests of this camera chamber were made with 16mm. Tri-X film. The film was held on the film plate by double sided Scotch tape. In a typical test, the film would be positioned in place, it would be exposed under prescribed conditions, and then moved about

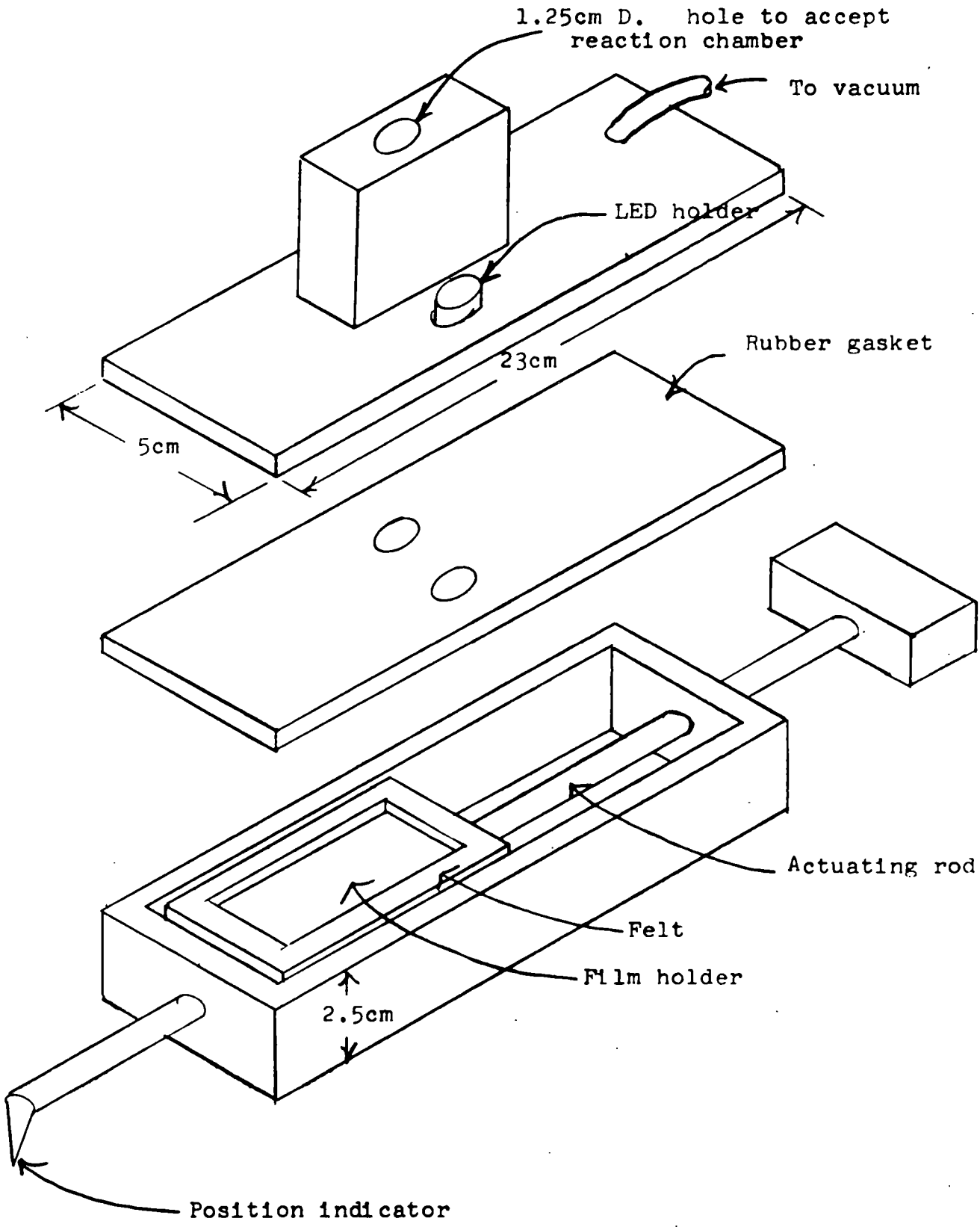

Figure 2 Chemiluminescent Camera

1/4 inch to a new position where different exposure conditions were used. The film was moved between each exposure until all tests were completed or until the entire film strip was used. Development by Microdol-X (according to the manufacturer's recommended procedures) always immediately followed the last exposure.

The MV-1 LED produced an image 1.1mm. in diameter for very low light levels. Higher light levels resulted in a central dense spot about 1.1mm. in diameter, surrounded by a 5mm. diameter spot having about one-third the density of the central spot. The values shown in table 4 indicates some of the relative densities obtained under varying conditions. The equivalent ozone values were obtained as before by

TABLE 4

Tri-X Sensitivity

LED CURRENT	Equiv. Ozone	Exposure time	Relative Density
1 uA	0.18 ppm	20 min.	0
2	0.7	20	1
4	2.6	20	3
8	9.5	20	6
1	0.18	60	0
2	0.7	60	3
3	1.6	60	5

determining the Meloy PMT response to varying currents through the LED. The relative density values were subjective appraisals on a 0-10 scale where 0 indicated no perceptible image. It may be seen that a light exposure equivalent to 0.18 ppm ozone produced no image, even for 60 minute exposure times. Increasing the exposure time from 20 minutes to 60 minutes resulted in a marked increase in density for the same exposure levels, and a decrease in the exposure level required to produce a given density. This indicates that Tri-X has reasonably good reciprocity characteristics. This is in marked contrast to prior

results with Polaroid 3000 film where a 60 fold increase in exposure time only resulted in a 2-fold improvement in sensitivity.

The results shown in table 4 indicate that the minimum threshold level for Tri-X film is about 0.3 ppm ozone for a 1.1 mm. spot, or approximately 30 ppm/cm^2. This is essentially the same as was found for Polaroid 3000 film. Since this film also has a "flat" spectral response characteristic, it's true sensitivity also is 20 times poorer (due to the poor response of the PMT to the light wavelengths emitted by the LED). This "true" sensitivity then becomes 600 ppm. ozone/cm^2. Clearly then, even with reasonable good photographic films, the entire chemiluminescence reaction must occur within an area of 10^{-4} to 10^{-5} cm before photographic film can be comparable to PMT's.

4.5 Reaction Chember Tests

It was previously shown that the chemiluminescence must be concentrated in a very small area if adequate sensitivity is to be achieved with photographic film. Theory dictates that it is impossible to concentrate light by simple optical lenses or mirrors. Some preliminary tests with lenses, mirrors, light guides, verified that normal optical concentration techniques were useless. One possible optical concentration technique would be to collect light emitted within a glass sphere with fiber optics arranged in "porcupine" fashion. The fiber optics could then be bent and arranged in a single bundle, thereby creating a rough collination of the heretofore diffuse light. This collimated light could then be concentrated by conventional optical methods. The mechanical problems associated with this concept would be exceptionally severe and it did not appear warranted to follow this path.

It was shown that the chemiluminescense reaction must be concentrated in an area of approximately 10^{-4} to 10^{-5} cm^2. This is equivalent to a circle 0.04 to 0.11 mm. in diameter. Since this small size precludes a spherical reaction chember, a long tubular-shaped chamber was dictated. Although the fact that the Meloy chamber exhibited marginal mixing behavior even though it had a very large size was discouraging, we proceeded with the development of smaller reaction chambers. The first chamber had a 0.76mm O.D. teflon tube with a 3.2mm O.D. x 1.52mm I.D. teflon tube that opened 15 mm back of the viewing port. This pair of tubes was inserted into a tube that could be evacuated and had a #0 cover slip as its window. All joints were sealed with silicone rubber. This chamber was positioned against the PMT. Various air flows and ethylene flow rates were tested. The ethylene flow rate had only slight influence on a signal. The signal response was essentially linear with the reciprocal of the air flow rate. Using the inner tube for ethylene and the outer tube for air gave about 50% greater response than the reverse case.

When this reaction chamber was operated under identical conditions to those used for the Meloy chamber, a reading of .004ppm ozone was obtained. With the smaller area of the new chamber ($1.8mm^2$ vs. $284mm^2$), this represented an intensity per unit area improvement of 3.0.

In view of the relatively poor improvement shown by the new chamber, some basic diffusion parameters were calculated using Fick's principles. These are shown in table 5. The first column lists various flow rates, while the second column indicates the degree of mixing occurring between ehtylene and air. For example, a flow rate of 105ml/minute would mix 10% of the gases. It is obvious that the normal flow

rate of one liter per minute is responsible for less than 1% mixing efficiency.

TABLE 5

Diffusion Rate Parameters for a 1.5mm I.D. by 10mm Long Tube

Flow Rate Requirement	Mixing Homogeneity
7.4ml/min	99%
15	90
42	50
105	10
280	1

Since it appeared that a variety of tests would be needed before a small chamber that provided adequate mixing could be obtained, a more versatile chamber was built. This is shown in figure 3.

In operation, the smaller assembly was inserted through the rubber grommet until it touched the cover slip. The large housing could be mated with either the PMT or the camera. The 1.45mmO.D. tube was used for ethylene. This tube was considerably longer than its outer telescoping tube so that its end position could be varied without disassembling the chamber. Although ethylene flow rates were varied with all chambers tested, no large differences were ever noted. Consequently, a standard ethylene flow rate of 28ml./min. was used for all tests.

In the first test, the ethylene tube was positioned 4.0 cm. back of the outlet. When a one liter per minute air flow rate was used with the ozone generator on, a reading of 0.078ppm ozone was obtained from the PMT. After a mask with a 4mm D. hole was used to block out all but the tube itself, a reading of only 0.018ppm was indicated. This indicated that the bulk of the reaction was occuring after the

Figure 3

Chemiluminescence reaction chamber

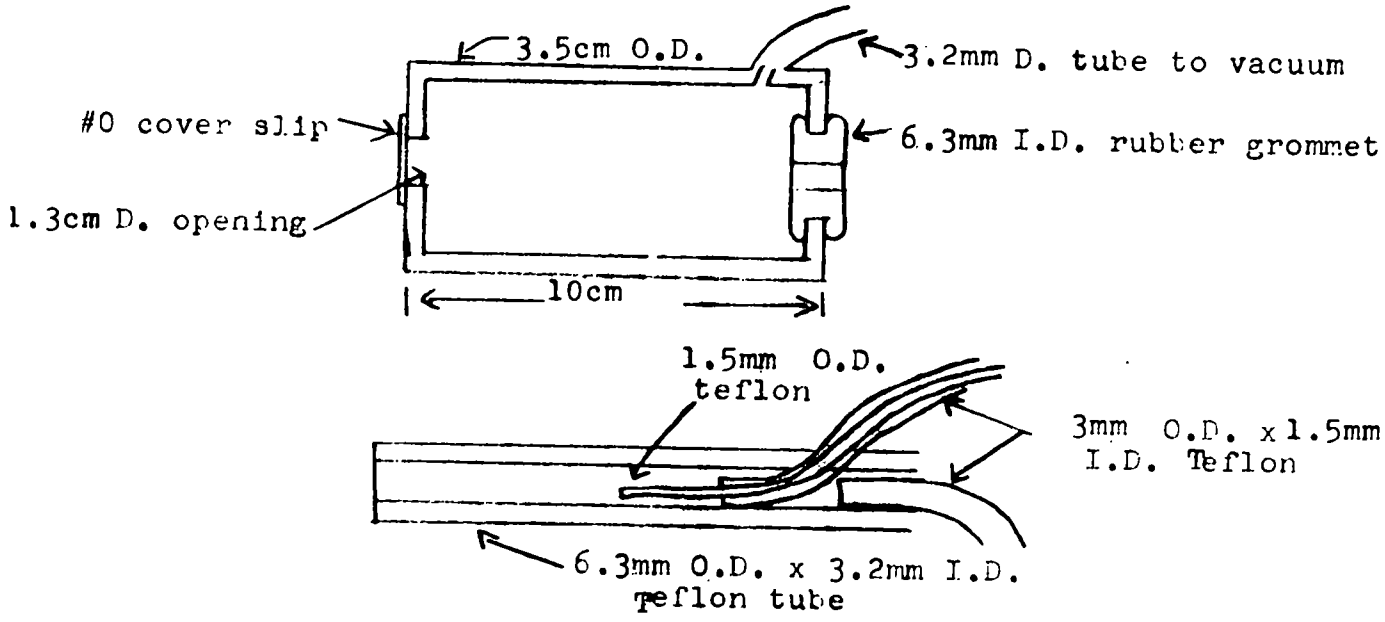

gases had left the reaction tube.

The relationship between air flow and ozone reading for this 3.3mm I.D. Teflon tube configuration is shown in figure 4.

It may be seen that a very linear relationship was obtained between the reciprocal of the air flow and output signal (as with the Meloy chamber). A 3.0mm I.D. aluminum tube inserted into the chamber did not change the values, thereby indicating that it was not sufficiently reflective to exhibit light-piping effects, or sufficiently reactive to increase ozone consumption. Results of the previous 1.5mm I.D. teflon tube chamber also are shown in figure 4. Since this chamber had more light attenuation as well as a greater gas velocity, its light output would be expected to be less.

The other two "orifice" curves in figure 4 are of greatest interest. In these cases, a 3.0mm O.D. by 3.0cm. long by either 1.5mm I.D. or 0.76mmI.D. was inserted in the throat of the chamber. The ethylene tube was moved just back of the insert. Both of these curves exhibited increasing signals with decreasing flows at high flow rates, but then reached a plateau at the lower flow rates. This probably indicated complete consumption (due to complete mixing) of the available ozone. The smaller orifice had a lower signal probably because of optical attenuation. It also required a lower flow rate before the plateau was reached, presumably because of the higher velocity characteristics of small tubes.

When data are plotted against the reciprocal of the air flow rate as in this case, it is really analogous to plotting the data against ozone concentration, since the ozone concentration decreases as the air flow increases. Although it may appear that a straight line

Figure 4

Effect of gas velocity on signal

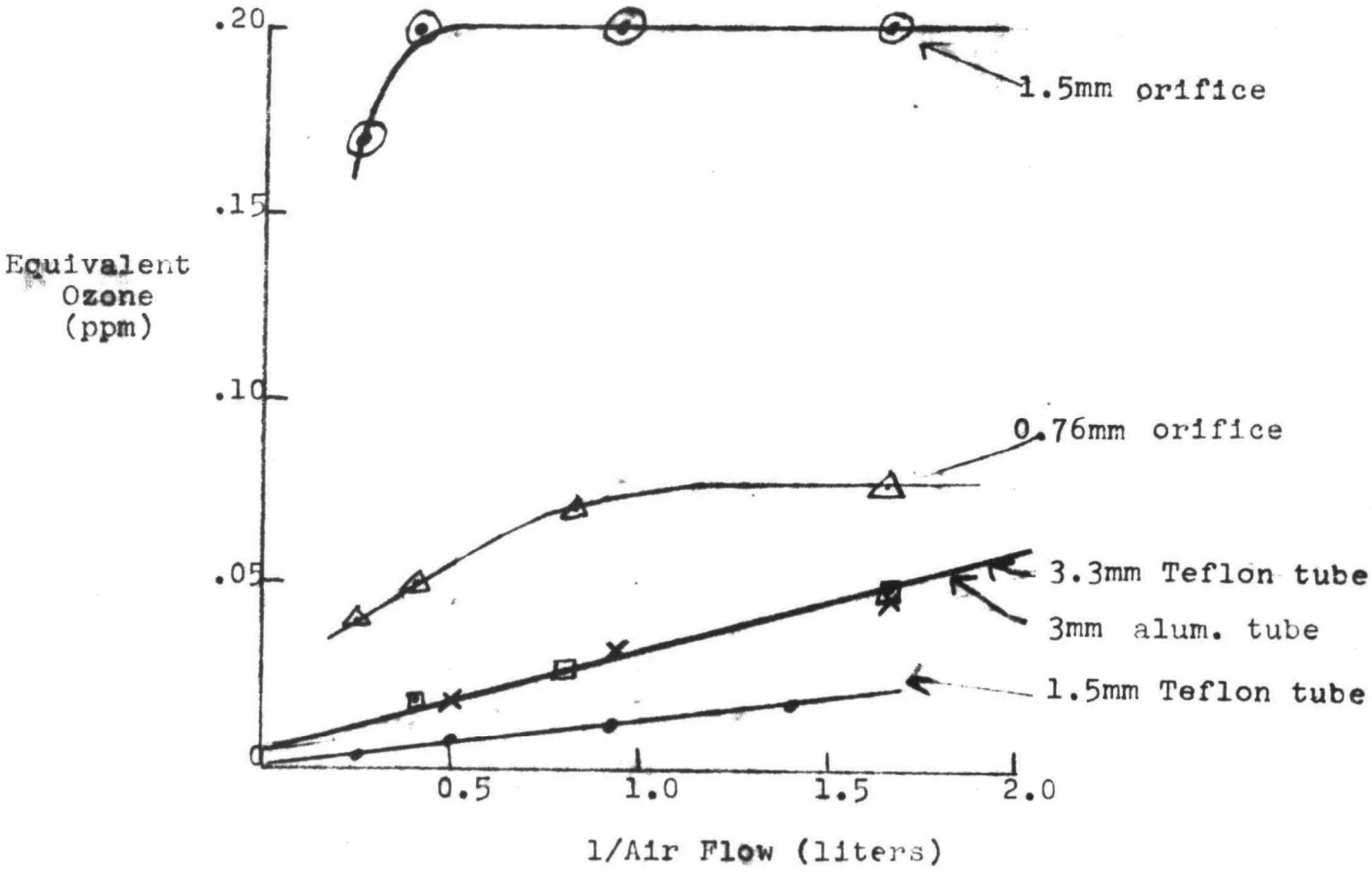

function should occur with no plateau, this is not the case if efficient mixing occurs. The correct model for this type of test is to assume that there are three gas flows - ethylene, pure ozone, and air. Since the ozone generator produces a constant flow of ozone regardless of air flow, the air merely serves as a diluent. Consequently, under complete mixing conditions, one would expect a constant response regardless of air flow rate.

The preceding data are tabulated as a function of chamber area in table 6. In all cases, the values obtained at an air flow rate

TABLE 6

Relative Intensity Obtained
from different reaction chambers

Type of Chamber	Diameter	Ozone Reading	Reading/ Diameter^2	Relative Intensity
Original	1.95mm	.22ppm	0.06	1.0
Teflon tube	1.5	.004	0.17	2.8
Teflon tube	3.3	.017	0.16	2.6
Aluminum tube	3.0	.017	0.19	3.1
3cm long orifice	1.5	.20	8.6	113
3cm long orifice	0.76	.05	8.6	113

of one liter per minute were used. It may be seen that the straight tubes provided an intensity increase of about 3 regardless of diameter or material. The orifice tubes which provided a turbulence-producing edge, had 113 times as great a light intensity as the original tube. The 1.5mm inch orifice chamber had essentially the same total quantity of light as did the original chamber. In view of the large signal as well as the plateau formation (fig. 4), we can safely assume that essentially complete reaction is occurring. The 0.76mm inch orifice tube did not show the expected 4 fold increase in intensity. Since the air flow curve shape indicated complete mixing, this lack of additional improvement simply was due to loss of available

light due to the small hole. In spite of the 100 fold intensity improvement, it was still not possible to obtain a photographic image.

If one assumes that the average light-producing collision occurs in the middle of the tube (1.5cm back of the viewing port), the viewing angle even with perfectly straight chamber walls is only 6° and 3° for the 1.5mm and 0.76mm chambers, respectively. This corresponds to a total light gathering efficiency of only .025% for the 1.5mm chanber, and .006% for the 0.76mm chamber.

Other chamber lengths and ethylene tube placements resulted in either the same intensity or decreased intensity. An interesting observation was that a significant ozone response was found for as long as three hours after the ethylene was turned off. With the smaller orifice chamber, this response was essentially the same as when the ethylene was on. Extensive flushing of all ethylene tubes with air immediately after ethylene shut-off did not alter this situation. It thus appears that ethylene probably is being absorbed in the tubing, and exceedingly small quantities of ethylene are required if a well designed chamber is used.

The next step was to explore the possibility of utilizing internal reflectance in order to increase the light gathering efficiency. It was hoped that reaction chambers with good internal reflectivity properties would permit the use of longer tubes (for better mixing) and smaller diameter tubes (for better light concentration).

A series of tests were made to determine the reflectivity properties of various tubes. A controlled diffused light source was oriented at one end of the tubes, while the Meloy Labs PMT was used at the

other end to determine relative light intensity values. Twelve inch tubes were tested in all cases. Results of these tests are shown in table 7. The first column lists the type of tube tested, the second column indicates the inside diameter, the third column shows the amount of light passed by the tubes (in equivalent ppm ozone), and the last column relates the average light intensity per unit area. It may be seen that the glass tubes gave the best results, with the small bore capillary providing an intensity gain of 34 fold. If we assume a critical angle of 30° the increase in light intensity should have been a factor of 40,000 gain. The relatively low gain could be accounted for if the glass only reflected an average of 96% of the light with each bounde. Although a factor of 34 gain can be achieved, much higher gains are possible if the average reflectivity could be increased above 96%. However, this may not be practical for a field instrument.

The calculated efficiency for the small bore tube is about 0.1%. If we take a rather simplistic view and assume that the average chemiluminescent collision occurs in the midpoint of the tube, the overall efficiency should be 3.2%. A 30cm long by 0.5 mm reaction chamber should then exhibit an improvement of $.032/.05^2$ or 12.8 fold over a one cm^2 chamber.

In order to evaluate actual chamber performance, various tests were made with small bore capillary tubing. The 6.3mm O.D. x 0.5 mm I.D. capillary tube was mounted in a 13mm vacuum tube equipped with a #00 cover slip and a suitable adaptor for mounting on the photomultiplier tube. Air and ethylene were mixed right at the entrance to the tube. Ethylene flow rates of 0.25, 0.5, 1.0, 1.5, and 2.0 liters per minute

TABLE 7

Relative reflectivity of various tubes

Type of Tube	Inside Diameter	Light Intensity	Relative Intensity per $mm.^2$
None-holes spaced 30cm apart	1.8mm.	1.35	1.0
Teflon	.75	.74	3.0
6.3mm O.D. glass	.50	3.80	34
1.5mm O.D. glass	1.0	4.30	10
Stainless	1.1	.87	1.6

were tested. Three different tube lengths - 23, 30, and 53cm tested. Results of these tests are shown in figure 5.

In all cases, the lower ethylene flow rate showed a moderate decrease in sensitivity. The 23cm chamber had very good response but the plateau was not as flat as previously experienced with larger diameter chambers. This indicates that complete mixing is not occurring in the tube, and longer tubes are indicated. The 30cm chamber still didn't have a flat plateau, and had considerably less response than did the 23cm chamber. The lower response is due to greater reflectance losses. These losses are further indicated in the 53cm chamber. Here, only the very high flow rates gave a signal. At normal air flows, the reaction apparently occurred so far down the tube that its light was completely absorbed before reaching the PMT.

Both the 23 and 30cm reaction chambers showed better response than would have been indicated by the internal reflectance tests. Whereas the reflectance efficiency for the 30cm had been calculated at 3.2%, the actual response was roughly 50% as great as the original Meloy chamber. This discrepancy probably is due to a better mixing efficiency in the capillary tube than the Meloy chamber, since the Meloy chamber never has shown any plateau characteristics on a response vs. velocity plot. Other possibilities are an underestimation of the reflectivity (a 1% error in the estimated reflectance per bounce would have a large effect on total efficiency) or to the bulk of the reaction occurring forward of the tube's midpoint. In any case, the test results looked very encouraging. If we compare the response per unit area of the 23cm tube (0.5mm I.D.) with the original Meloy chamber (19mm I.D.), we find a net decrease in area of 1,400 fold coupled with

Figure 5

Effect of reaction chamber length

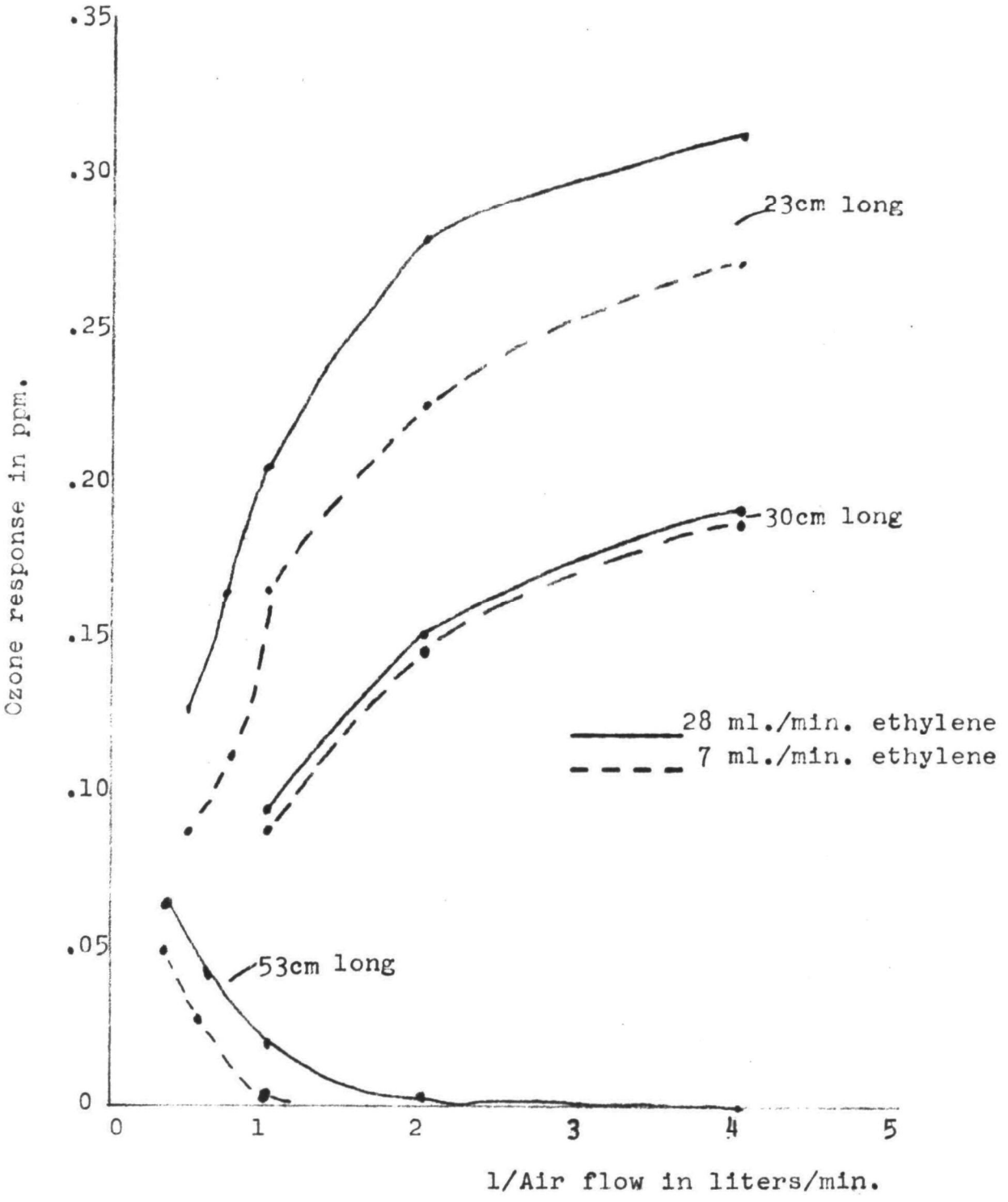

only a slight decrease in total response. Thus, the brillance was increased 1,000 fold. In comparison to a one cm^2 area cell, brilliance was increased approximately 250 fold. Since previous calculations had indicated that the brilliance of a hypothetical $1cm^2$ area chamber must be increased by between 10^4 and 10^5 before photographic film would be comparable to a PMT, we were still approximately two orders of magnitude away from our goal. Since the use of even smaller diameter reaction tubes would begin to pose serious pressure drop, mixing, and plumbing problems, we decided to terminate any further work on smaller chambers and concentrate on the photographic film aspects.

Various capillary tube reaction chambers including the 23cm 0.5mm I.D. tube, a 7.6 by 0.1cm I.D. tube, and others were used in conjunction with various photographic films. These films included Polaroid 3000, Tri-X, and Ia-0. Exposure times up to 4 hours were used, and all developing was by manufacturer's recommended procedures. Air flow rates and ethylene flow rates were varied over wide ranges. The Meloy ozone generator (0.3ppm ozone) was used in all tests, and proper operation was confirmed by checking light emission with the Meloy PMT prior to each series of photographic tests. In no instance did we obtain any perceptible images on the films. Even optical coupling of the capillary reaction tube to the surface of the film (by using appropriate quartz lenses) did not yield any images. These results merely confirmed the theoretical calculations which stated that several orders of magnitude more sensitivity was still needed. In view of the increasing difficulty of obtaining additional significant sensitivity improvements, this approach was terminated. Perhaps the future will

yield films with better sensitivities (some of the newer solid state image storage plates already look promising). In that event, the present work on improved mixing efficiency and smaller viewing areas should prove valuable.

4.6 Gas Permeation Studies

Even though the photographic film recording approach had not proved fruitful, the use of small capillary tube reaction chambers had opened up the possibility of using gas permation rather than direct injection of ethylene into air.

One of the major logistic disadvantages of chemiluminescent ozone analyzers is the necessity to supply ethylene. If this could be replaced by a reactive liquid whose vapors diffused into the chamber, a much simpler system could be developed. Consequently, the feasibility of using a diffusion membrane was tested.

Figure 6 describes the test setup used. The air flowed past the silicone rubber tube, through the capillary tube, and to the vacuum port. The ethylene was allowed to flow at 15ml. per minute through the reservoir surrounding the diffusion tube. Response dropped severely when ethylene flow was stopped, presumably due to rapid depletion. The diffusion device was tested against direct injection of ethylene into the end of the capillary tube. The results are shown in table 8.

Table 8

Effect of Diffusing Ethylene into the Reaction Chamber
(Responses given in equivalent ppm. ozone)

Air flow rate	Ethylene @ 28ml./min.	Ethylene @ 7ml./min.	Ethylene diffused in
2.0lpm	.110	.095	.075
1.5	.145	.120	.090
1.0	.190	.165	.120
0.5	.275	.245	.175
0.25	.280	.265	.170

Figure 6

Gas permeation tube test

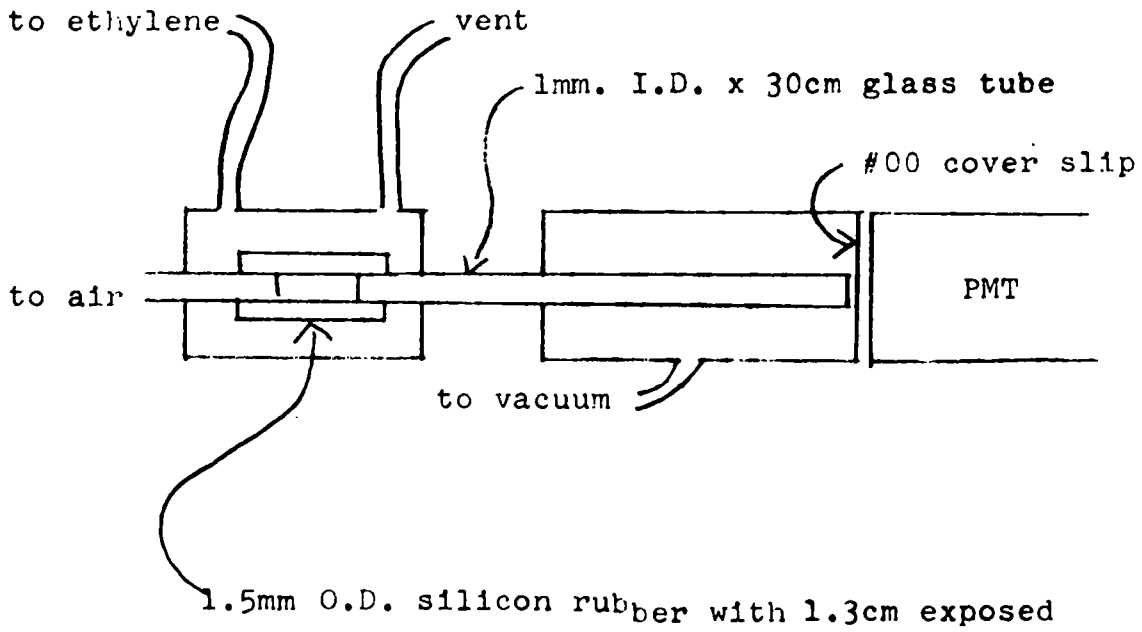

In all cases, the usual pattern of increasing response with decreasing air flow, finally reaching a plateau, was found. The response decreased about 10% as the ethylene flow was reduced from 28ml./min. to 7ml./min. With the diffusion device, response dropped another 30%. Nonetheless, the response obtained by diffusing ethylene through silicone rubber was quite respectable. It opens the possibility of diffusing liquid reactants, thereby eliminating the gas bottle requirement.

4.7 Direct Air Injection

Film manufacturers have a problem of film fogging due to the chemiluminescence reaction of ozone in the atmosphere with gelatin. In order to overcome this problem, they use sealed shipping containers and add antioxidants to the film. It was attempted to use this reaction as the basis of an ozone detector.

One end of a 3.2mm Teflon tube was connected to the ozone generator and the other end was positioned about 3.2mm from the film plate. Vacuum was applied to the camera case to create a flow rate of one liter per minute. No reaction with Kodak Tri-X 16mm. film could be found after one hour exposures.

In other tests an air pump was connected to the ozone generator inlet, and positive pressure was used to direct a one liter per minute air flow onto the film. Again, no exposure could be seen after development

It thus appears that either the 0.3 ppm ozone concentration cannot overcome the antioxidant, or the one hour exposure time is much too short. In any case, this does not appear to be a fruitful approach.

5.0 Alternative Detectors

Even though the direct film exposure concept proved to be unfeasible, a drastic need still existed for a reliable, low cost, long term recording monitor for air pollutants. Although the chemiluminescence reaction itself is simple and reliable, the extremely low light emission level has made it necessary to use photomultiplier tubes as sensors. The gain as well as zero level of PMT's is markedly altered by changes in temperature and voltage. Consequently, a portable instrument would require a thermostatted oven (very high power consumption), and a very well regulated power supply (expensive). In an effort to overcome these disadvantages, various other photodetectors were tested.

In most cases, the test setup consisted of an 24v. power supply with 1.5 Kohm, 1.2 Kohm, 1.0 Kohm and 820 ohms current limiters (positions 1,2,3,4), driving a 24v tungsten filament lamp. The lamp was optically coupled to the detector under test through a 24 inch quartz fiber optic tube and a Wratten 36 filter. This provided varying light intensities at a wavelength of 420nm with a half-band width of 45nm. In addition, a Schott BG18 filter was used to exclude infra-red light in tests of the solid state detectors.

Results of the photodetector tests are shown in table 9. The first column lists the detector while the second column indicates the test conditions. In most cases an electrometer amplifier was used to measure current output, but the Meloy Ozone Analyzer also was used in several cases to obtain a correlation between current and ozone readings. The last five columns list the outputs obtained under dark conditions, and four different lamp intensities.

TABLE 9

Response of Various Photodetectors

Detector	Test Condition	Dark	Lamp 1	Lamp 2	Lamp 3	Lamp 4
Heloy PMT	Ozone amplifier, 1200v.	0ppm.	0.3	5.5	Overrange	
Heloy PMT	Electrometer, 1200 v.	0uA	.01	.13	1.38	3.18
RCA 1P28 PMT	Ozone amplifier, 800v.	0ppm	.01	.086	.25	1.40
RCA 1P28 PMT	Electrometer, 800v.	1.37na.	1.43	1.85	2.75	8.72
CL902L	Electrometer, 15v.	2.00na.	2.01	2.04	2.05	2.25
PD 1900-S4	Electrometer, 15v.	25.0pa.	25.2	25.2	28.0	29.0
PD 1900-S10	Electrometer, 15v	42.0pa.	42.0	42.0	43.0	44.3
DT 1737	1 Meg x 1000 (1mv=1pa.)	44.7pa	-----	46.7	49.7	83.0
CLR 2060	Electrometer, 1v.	1.85na.	1.85	1.87	2.09	2.31
CLR 2180	Electrometer, 1v.	6.53na.	6.53	6.67	6.77	21.1

The first test with the Meloy PMT showed the correlation between our simulated light conditions and the chemiluminescent light emission. The actual current output of the Meloy PMT was directly related to the ozone reading. The 1P28 PMT had considerably less response than the Meloy PMT. This would be expected in view of the lower operating potential. The Clairex CL902L cadmium sulfide photoresistor tracked the simulated light conditions almost as well as the 1P28. It had a higher relative dark current and its response was exceedingly slow.

The next three detectors are vacuum photodiodes manufactured by the Tung-Sol division of Warner Electric Corporation. The PD 1900-S4 appeared to follow the light source somewhat, but the signal to dark current ratio was very poor. Also, the current increase equivalent to 5.5ppm ozone was only 0.2 picoamperes, which makes it difficult to design suitable amplifier circuits. The PD 1900 with S10 response characteristics gave even poorer response, presumable due to its greater sensitivity to red light, which is a noise and dark current producer in this application. The DT 1737A is a PD1900-S10 photodiode coupled to a FET amplifier. It is advertised as being equivalent to photomultiplier tubes. Our tests indicated that it did indeed follow our simulated signals, but that its noise and drift characteristics were unacceptable.

The CLR 2060 and CLR 2180 detectors are silicon photodarlingtons sold by Clairex. They differ only in that the CLR 2180 has a lens to collect light. Even though these detectors have maximum sensitivity to 900nm light and only about 5% as much sensitivity to 400nm light, both detectors were able to measure light intensities equivalent to 5ppm ozone or greater. In going from darkness to lamp 4, CLR 2060

increased by 0.46na. while CLR 2180 increased by 14.6na., thereby showing the importance of good light collecting ability.

The preceding results cannot be strictly related to detectability of chemiluminescence because of their disproportionate sizes. Since these tests were made with a small diameter (3.2mm) light source, all detectors collected a high proportion of the available light. With a large diameter (over 2.5cm) reaction chamber as used in the Meloy ozone analyzer, only the Meloy PMT (which has an end-on configuration) will collect the light efficiently. The 1P28 PMT, which has a side window configuration collects less than one percent of the light. No signals due to the ozone reaction were obtained with the 1P28. The vacuum photodiodes would collect about 20% of the light but their responsivity characteristics are poor. The solid state detectors collect very small proportions (less than 0.1%) of the light and have poor responsivity characteristics. It was concluded that only end-on photomultiplier tubes are capable of monitoring the ozone-ethylene chemiluminescent reactions at this time.

6. Photon Counting

6.1 General Background

All light originates as discrete energy particles termed "photons". The eye, most detectors, and most amplifiers are too slow to respond to individual photons. Consequently, the output of most photodetectors appears to be an analog signal, the magnitude of which is proportional to light intensity. With a sufficiently fast response system (risetimes less than one microsecond), the detector output appears as a number of sharp spikes, each of which represents a single photon. The height of

the spikes remains constant regardless of light intensity. Increased light only results in increased numbers of spikes.

A recent article by Zatzick (1) reviews the advantages and general state of the art of photon counting. Photon counting is universally agreed to be the ultimate method for obtaining the best reliability and signal-to-noise ratios in low light level applications. In photon counting only the number of photons are counted. Electronic noise is eliminated by threshold circuits and dc drift is eliminated by using ac coupled amplifiers. With conventional analog systems, not only the number of photons affect the signal, but also their peak height, the frequency of cosmic rays, electronic noise, and electronic drift. The apparent photon peak height is governed by the gain of the photomultiplier tube and amplifier. Although amplifier gain is stable, photomultiplier gain is greatly influenced by power supply voltage and is moderately influenced by temperature. This means that a very well regulated power supply must be used, and a controlled temperature oven must be provided for the PMT if it is used in the field. Cosmic rays strike the photomultiplier tube at a rate of approximately one/cm^2/sec. Since they are orders of magnitude larger than photon signals, they can have an appreciable effect on the baseline at low light levels. Electronic noise is another source of baseline drift. Although it is simple to remove this source of error by threshold limiting with a photon counting circuit, it becomes an appreciable signal in analog circuits. Electronic drift of both the PMT and amplifiers is an exceedingly difficult problem to solve with standard analog circuits.

1. Zatzick, M.R. Electro-Optical Systems Design, June 1972, pp. 20-27

Photon counting circuits always are AC coupled so as to eliminate this problem. Thus, the photon counting technique eliminates many error sources which limit the sensitivity and reliability of conventional systems.

6.2 Electronic Considerations

6.2.1 General

Although photon counting has many theoretical advantages over standard analog integration procedures, the electronic circuitry must be relatively sophisticated to avoid introducing new problems. Fig. 7 illustrates the basic components required to monitor chemiluminescence reactions by photon counting techniques. A photomultiplier and its power supply are needed just as in an analog system. The pre-amplifier serves to lower the impedance of the signals. The comparator discriminates between the photoelectron signals and noise, and amplifies the photoelectron signals to a saturation level voltage. The divider network reduces the total counts to manageable levels, while the readout system permits a number representative of the pollutant level to be recorded. Perhaps the most difficult area is in obtaining adequate risetime speeds from the PMT amplifier. If the response speed is too slow, the photoelectron signals will appear as broad peaks instead of sharp spikes. This results in a poorer signal-to-noise ratio and in peak overlap at higher light levels. The peak overlap causes doublet and triplet photoelectron peaks to appear, which results in an exponential power of 2 or 3 relationship between counts and light intensity, instead of the normal linear relationship. The other major problem area is in handling the massive number of photoelectron counts. Since approximately 1000 photons must be counted each second, a 24 hour accumulation would result in

Figure 7

Basic components of the chemiluminescence photon counter

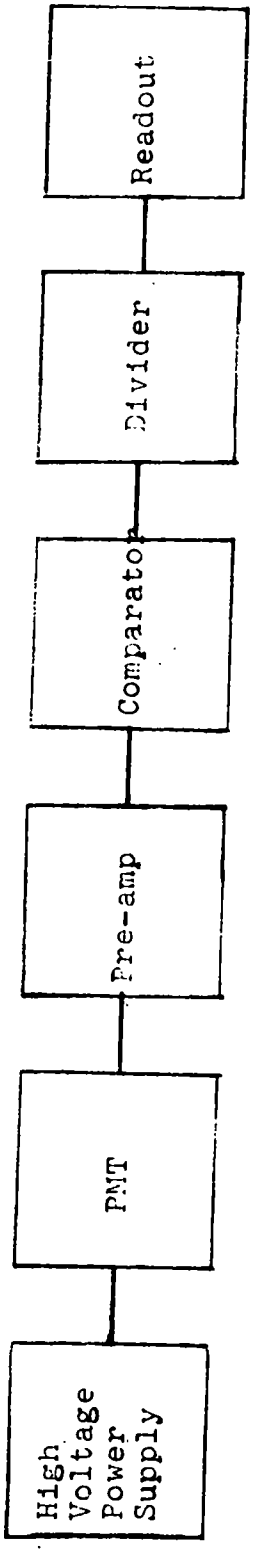

approximately 100 million counts. This is handled most easily by using a "brute force" approach of digital division.

6.2.2. Power Supply

The high voltage power supply can be relatively poorly regulated since amplitude changes of the photoelectron signals do not have a direct influence on the number of counts. The current capability of this power supply need be only one-tenth as great as required for analog systems, because the dividing chain can be composed of much higher resistance values. This is possible because each photoelectron places a constant current load upon the PMT, as opposed to the variable load imposed when the PMT is operated into an integrating current amplifier.

Almost all of the lower cost high voltage power supplies operate as dc-dc converters. The input d.c. power is chopped at approximately 10KHz, transformed to a higher voltage, and then rectified to obtain a high voltage dc output. The chopper frequency appears at the output as a ripple, which ultimately becomes noise. Since a photon counting system can discriminate against this ripple, it can tolerate the use of these low cost power supplies. All studies on photon counting were made with a Mil Electronics type VL15 power supply. This unit transforms input voltage to a voltage 100 times greater. It was normally operated with a 12vdc input and a 1200 vdc output.

6.2.3. Photomultiplier tube

Most of the requirements for a photomultiplier tube used for photon counting are similar to those for normal analog usage. In order to obtain best sensitivity and reliability, it should have minimal response to longer wavelengths, since longer wavelength response increases the thermionic noise problem. It should also have the minimum

possible cathode area, since excess cathode area increases thermionic and cosmic ray noise. DC leakage is unimportant for photon counting purposes, so dark current values are not especially meaningful. A special requirement is that the PMT must have fast response characteristics.

The EMI 9524S PMT was chosen for this application. This 30mm. end-on tube has an S-11 spectral response. It was primarily chosen for its overall reasonable characteristics, rugged construction, and low cost. It has a somewhat slow rise-time response of 18 nanoseconds, but this is adequate if only low light levels are measured. Even though this is a moderately small diameter tube much smaller tubes are available at higher costs. Alternatively, a magnetic focusing lens could be used to reduce the effective cathode diameter. This tube was used as is, however, since it fit the existing Meloy reaction chamber and permitted us to proceed immediately to the photon counting problem.

The dynode chain configuration used with the PMT is shown in figure 8. This is a relatively standard configuration except that the chain resistance is ten-fold greater than normally used, and capacitors are used on the last three stages to provide a more constant gain regardless of the photon rate. Higher resistance is possible with photon counting circuits because less current is required at the low light levels generally encountered. It should be noted that the plate is tied to ground through a 22K ohm resistor. This permits the output to be monitored either by the photon counting amplifier or by a conventional dc analog amplifier. This permitted us a high degree of flexibility in our experimental tests. A major disadvantage of this configuration is that the PMT shield must be tied to the high voltage supply. A much safer and lower noise configuration would be to tie

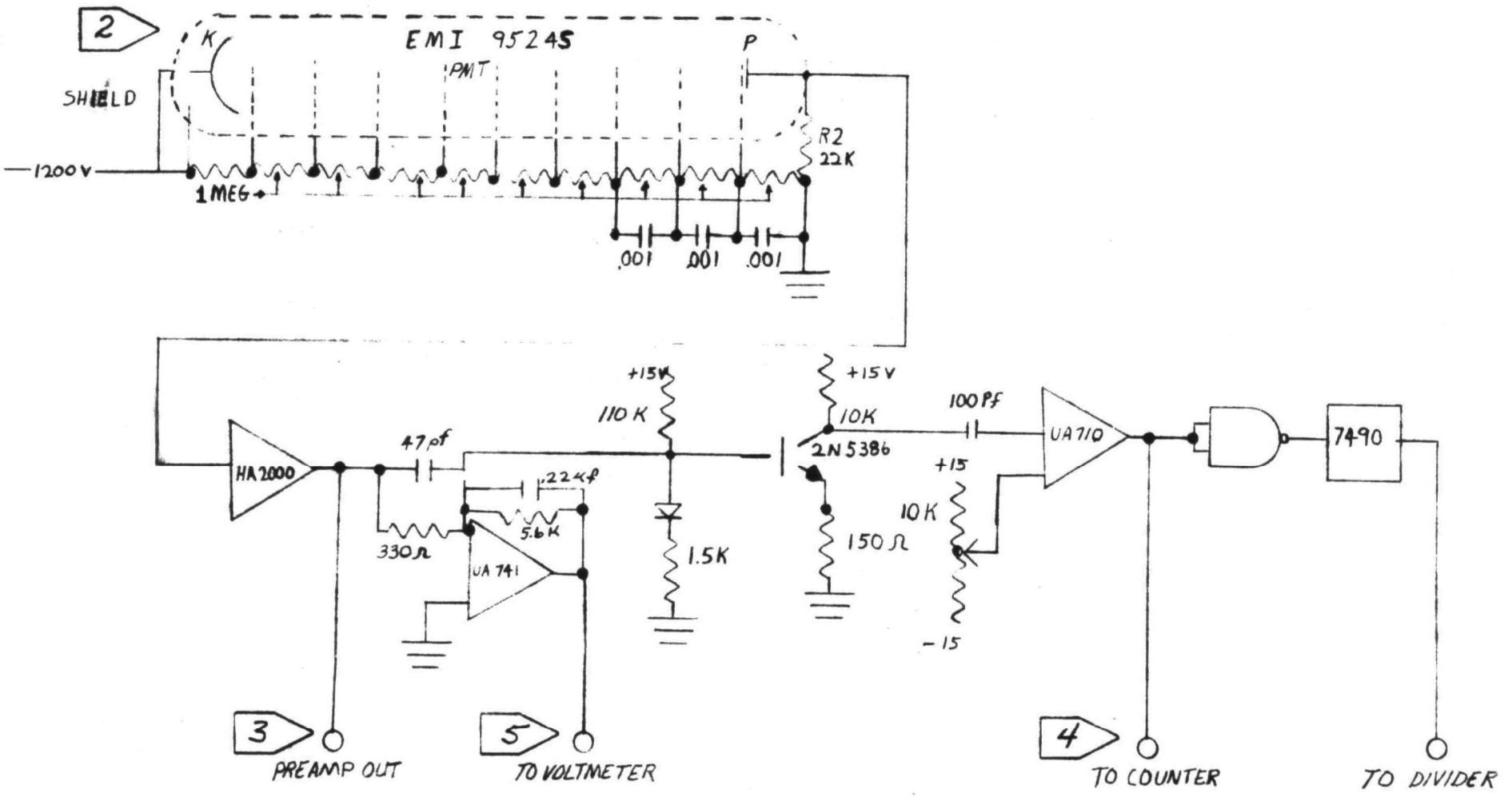

DENOTES APPENDIX B DESIGNATION

FIG. 8 PMT, PREAMP, AND COMPARATOR CIRCUIT

the cathode and shield to ground, and tie the load resistor to the positive high voltage output. This would necessitate an ac coupled circuit, which would preclude any dc current measurements. Nonetheless, if only photon counting were to be used, it would be recommended that the cathode and shield be grounded.

6.2.4. Amplifier Circuit

Also shown in figure 8 is the final amplifier circuit delivered in the breadboard instrument. The 22 Kohm load resistor was found to be the largest possible resistance that would not unduly broaden the photoelectron signals when unshielded wire was used between the plate of the cathode and the preamplifier. With the 22Kohm resistor, it was not possible to use shielded cables without broadening the signals due to the extra capacitance. This did not prove troublesome since shielded cables are not needed for photon counting purposes. The Harris HA-2000 preamplifier is a newly introduced FET input, unity gain amplifier which is capable of following 100 MH_Z signals. This preamplifier was very satisfactory and was used in all experimental configurations. A slow response amplifier was used at the output of the preamplifier so that EPA personnel could conveniently monitor dc current vs. photon counts. Very little work was done with this amplifier since we preferred to disconnect the PMT output lead and measure current directly whenever a comparison test was made. The auxiliary slow amplifier is completely functional and does reflect the true dc state of the chemiluminescent reaction. The output of this amplifier is quite rippled and drifts womewhat since this is typical of analog systems. The Meloy amplifier output appears smoother because it has approximately a 10 second time constant.

The output of the preamplifier also is fed through a coupling capacitor to an FET amplifier stage. A diode was used between these stages to prevent negative peak overshoot, which would unnecessarily increase peak doubling effects. This amplifier stage presented the greatest difficulties in achieving adequate speed and stability. Single transistors, as used here, are not thermally stable unless additional compensation circuitry is used. Integrated circuit amplifiers would be the ideal choice if available. Various amplifiers, including the LM101 with feedforward compensation and the Harris HA-2520, were tested in various configurations. In all cases, a linear relationship between current and count rate could not be achieved. Best results were obtained when the HA2520 was directly coupled to the HA2000 preamplifier in a standard two amplifier feed-back arrangement. Under these conditions, a power slope factor of 1.1 was achieved under low light level conditions. Even though the HA2520 has a very impressive slew rate of 120v/μs, the high gain demanded of this amplifier slows it to a point where response time is greater than one microsecond. This causes peak broadening, which results in some photon doublets that tend to degrade linearity (note: if only doublets were present, the photon count would be proportional to the square of the current).

In view of the poor thermal characteristics of the amplifier section, its output is capacitively coupled to the comparator. This comparator (a Fairchild uA710) is used with open loop gain so that any peaks exceeding a preset threshold value become amplified to the comparator saturation level. The comparator used in this circuit performed quite well. However, a far superior comparator has recently become available - the Advanced Micro Devices Am685. This comparator

has a 2ns resetime instead of the 40ns risetime of the μA710. Even more important, it has excellent stability (10μV/^{0}C. drift) which permits it to be used directly with very small signals. This makes it possible to couple it directly to the preamplifier, or to use an amplifier with low gain, thereby minimizing rise time. Thus, this comparator makes possible an amplification system made up entirely of stable temperature-compensated integrated circuits. Unfortunately, this comparator came on the market too late to be incorporated in our existing circuitry. This comparator uses ECL logic outputs instead of TTL as does the older 710 comparator. While this does not represent a difficult interface, it would have entailed making an entire new circuit board. Since the photon counting technique could be easily shown to be far superior to analog systems, the new comparator was not incorporated into the system.

The output of the comparator is available on an output jack labeled "counter". This makes it possible to use any standard digital counter to monitor the rate of photon production. The signal then proceeds to the "digital division" portion of the circuit, where the photon pulses are counted.

6.2.5 Digital Division

Figure 9 is a functional diagram of the decade division circuitry, while the complete circuit is shown in appendix A. The pulsed output of the comparator is fed to the array of decade dividers. Each stage performs a 10-fold division of the number of counts. Thus, a single pulse appearing at the output of the third decade divider would represent 1000 counts at the input. A rotary switch is used to select which decade divider output (the extent of division) shall be permitted to accumulate. The last decade divider outputs are decoded to binary

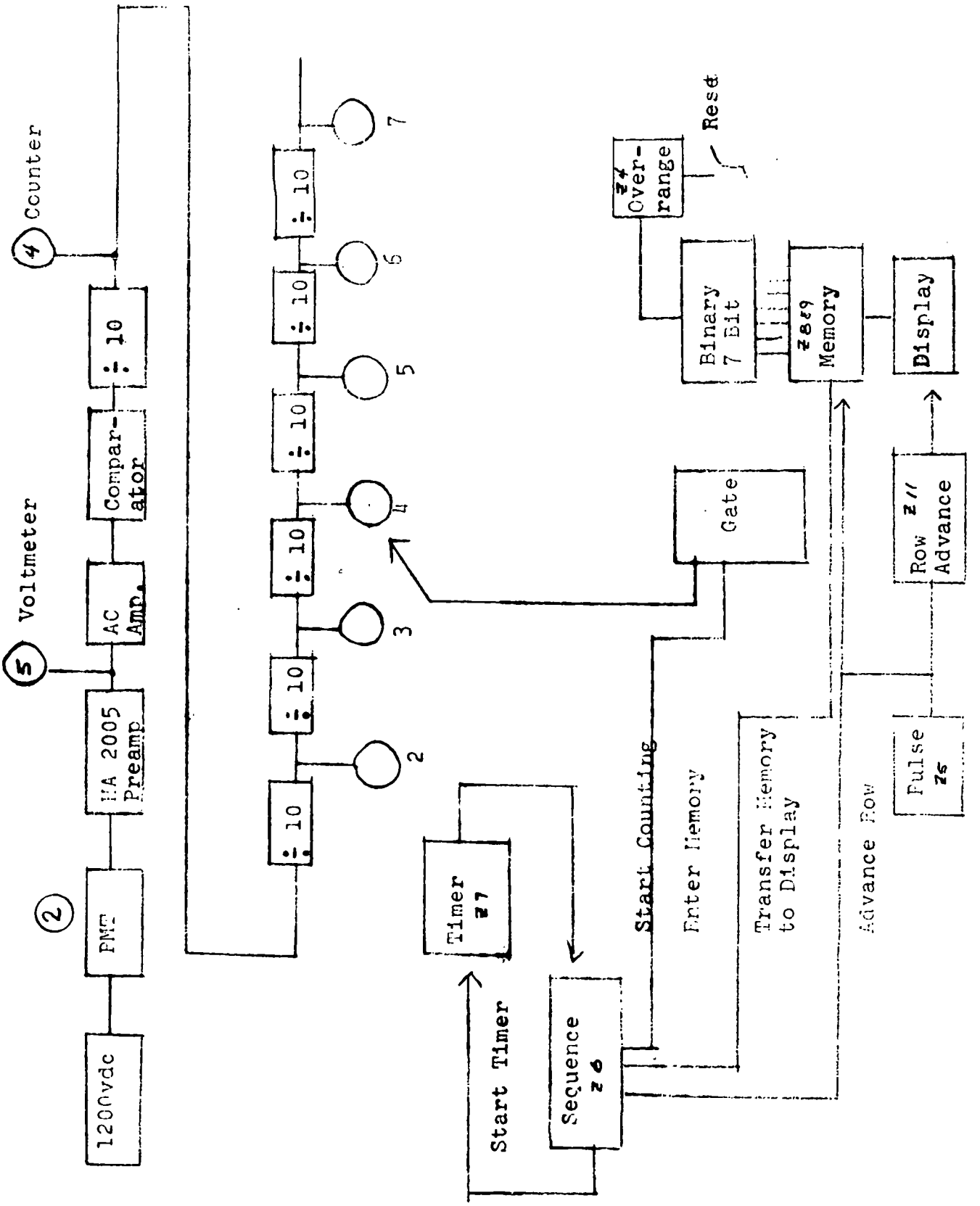

Figure 9

Photon Counter/Readout Circuit

form by a 7 bit binary counter. This counter provides a 7 bit parallel output that is related to pollutant concentration. This provides a resolution of one part in 127. Greater resolution is possible simply by using larger counters. The 7 bit accuracy was chosen since a 5x7 LED matrix was chosen as the readout device. Naturally, once the pulses are in digital form, any desired resolution can be obtained simply by using binary converters and displays with greater capacity.

The counting time is regulated by an RC network attached to a digital timer (SE 55). A rotary switch changes the timing period in decade steps from 0.1 minute to 100 minutes. At the end of each timing period, a number of events occur. These are:

1. Replace the previous counts in the memory with the accumulated counts from the last time period. These counts will be stored in the memory during the entire next timing period.

2. Advance the LED readout by one row and display the new counts during the next counting period. This results in a 7 bit number in one row of the LED display. This row is advanced during the start of each new timing period. In addition, the circuit shown in Appendix A also incorporates a "Blip" capability in which the LED matrix is dark during most of the timing period. The binary coded value only appears as a 0.1 second blip at the end of the timing period. If this is coupled to a photographic recording system, a very low power system can result.

3. Reset all dividers to zero. This readies them for the next timing period.

4. Reset the timer.

This logic system thereby results in a system in which both the amount of count division and counting time can be independently varied.

This degree of flexibility probably wouldn't be required in a field instrument, but it is helpful for R & D purposes. The 5 x 7 LED matrix displays a binary coded number that is proportional to pollutant concentration on one of its 7 bit rows. This display row is advanced one row at the end of each timing period in order to display the new reading. This system has functioned very well with no failures at any time.

6.3 Results

All data were obtained either by using the Meloy chemiluminescence chamber or by using a light bulb simulator having a filtered output of 410 nm. Photon counts were plotted against "ppm ozone" or against "analog output current" whose values were obtained by applying exactly the same experimental conditions while obtaining the analog or digital data.

When analog output currents were compared to photon counts, an extremely non-linear relationship was obtained in most cases (in early experiments). Reasonably linear relationships could be obtained in many cases if the count rate was raised to an exponential power between 1.5 and 3. Close examination of the photon shape on a Tektronix oscilloscope revealed that peak widths in excess of one microsecond were causing doubling-up of the photon signals. With the high speed circuitry shown in figure 8, however, good linearity was achieved in practically all cases.

A plot of photon counts vs. analog current is shown for various threshold level settings in figure 10. The count rate is displayed on the Y axis, while the equivalent analog current is shown on the X axis. The different curves are labeled according to the threshold

Figure 10 **Count rate vs. Current at various threshold levels**

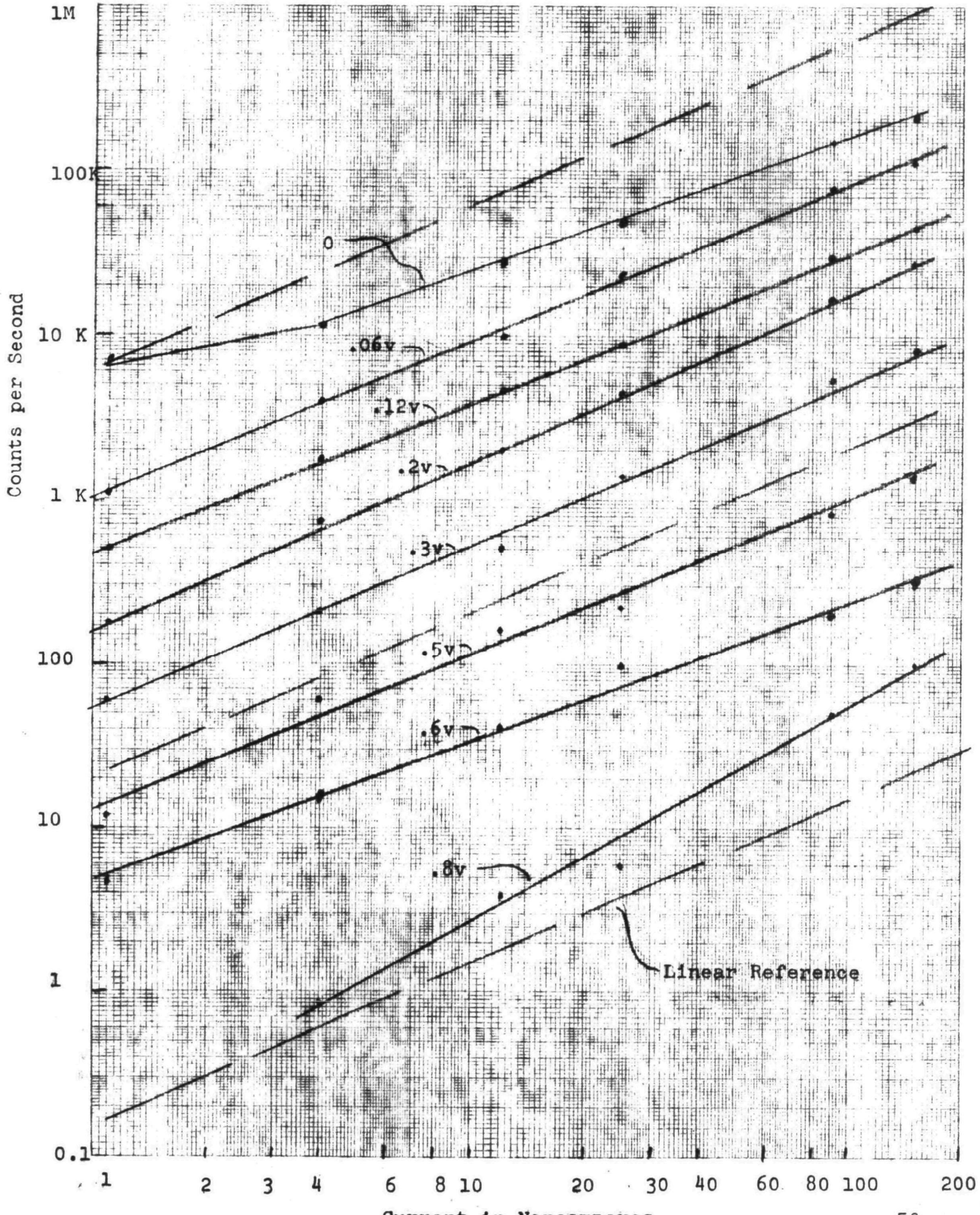

voltage applied to the comparator. Zero volts corresponds to essentially no threshold offset, whereby all counts are recorded. This curve has a slope less than unity because many of its counts are derived from electronic noise, which remains constant regardless of light level, thereby yielding a fairly horizontal slope. The 0.8v. threshold provided a slope greater than unity. This is presumably due to counting many "doublet" photon signals composed of two photon signals appearing at the same time, thereby yielding a signal twice as intense. All the curves obtained with threshold voltages between 0.06 and 0.6 volts are quite linear, thereby confirming the good high speed capabilities of the electronic circuit. From these data, it may be inferred that most of the noise pulses are smaller than 0.06 volts, and that most of the photon signals have amplitudes between 0.06 and 0.6v.

The data of figure 10 is reformated in figure 11 to show the relationship between threshold voltage and count rate for various light levels. As the threshold level is reduced from 0.06v. towards zero, the dark count rate increases very rapidly. This is due to counting electronic noise pulses near the zero threshold level. The region between 0.5 and 0.6 volts also is characterized by a steep slope. This is presumably due to a transition from counting only single photon signals to counting doublets. The region of least slope lies between 0.3 and 0.5 volts. This is presumably the peak height of the average photon signal. If the photomultiplier tube provided precisely the same gain for all photons, this region would be perfectly horizontal. If this were the case, the photon count would be completely oblivious to small changes in PMT gain. As it is, changes in PMT gain will affect the count rate, but much less severely than if it were operated in the

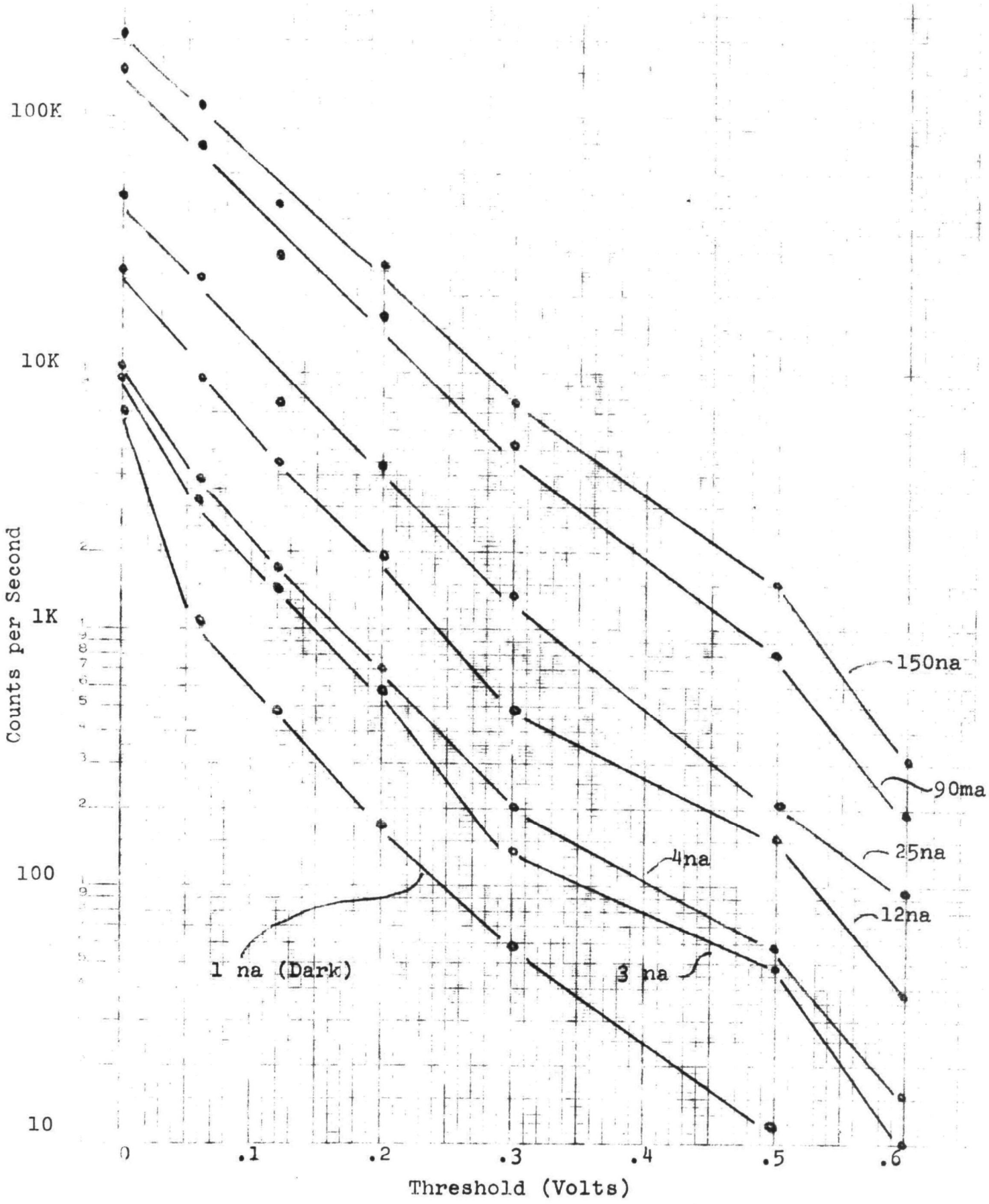

Figure 11

Threshold vs. Counts at Various Light Levels

analog mode. Better stability would be possible with gallium phosphide PMT cathodes which generate 30 electrons per photon. These PMT's are more expensive than the simple PMT used for these tests.

A plot of count rate vs. LED matrix readout is shown in figure 12. As would be expected with a digital system, a perfect correlation exists. A plot of PMT output current vs. ozone reading is shown in figure 13. This also shows a good linear relationship, as would be expected. The relationship between count rate and ozone concentration is shown in figure 14. A threshold setting of 0.2v. was used to obtain these data. It may be seen that very good linearity was obtained.

In summary, the photon counter exhibited very good linearity over a wide dynamic range. The threshold voltage setting for the comparator could be set between 0.06 and 0.6 volts and still achieve linearity. Lower thresholds settings tended to include electronic noise, while higher thresholds included primarily those photons that happened to appear at the same time as another photon. The primary known weaknesses of the present system - a cheap PMT and less than optimum analog amplification probably were responsible for a dependency of count rate upon threshold voltage setting.

7. Suggestions for future work

The feasibility of applying photon counting principles to chemiluminescence detectors has now been shown. Sensitivity is now limited only by thermionic noise - amplifier drift, cosmic rays, power supply drift, etc. create little or no interference. It is suggested that the already good performance of the present photon counter can be improved at least 10 fold by utilizing a small area detector to decrease the thermionic noise contribution. This will be especially important

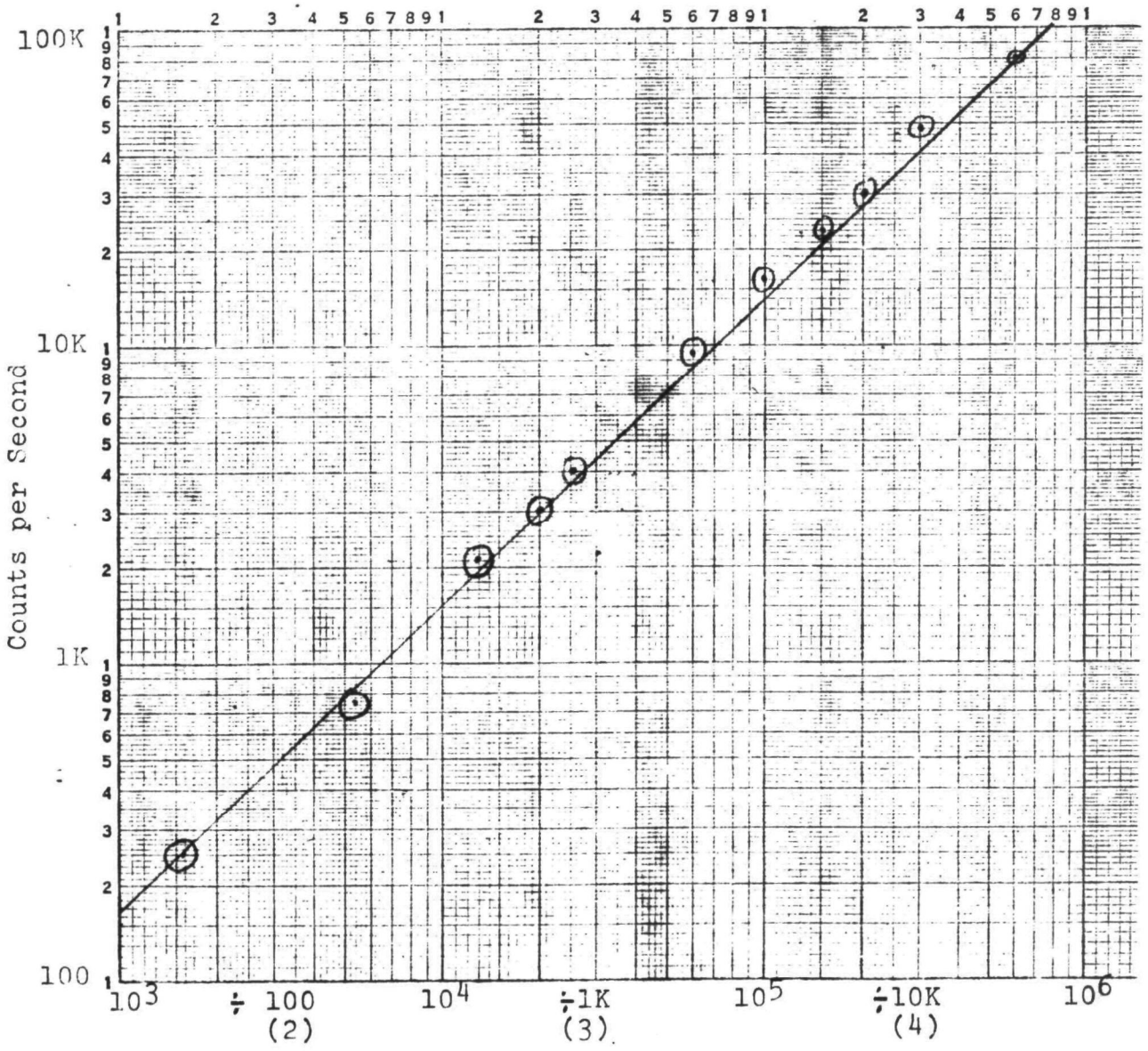

Matrix Readout
Time Base = 6 seconds

Figure 12 Correlation of Count Frequency with Display Reading

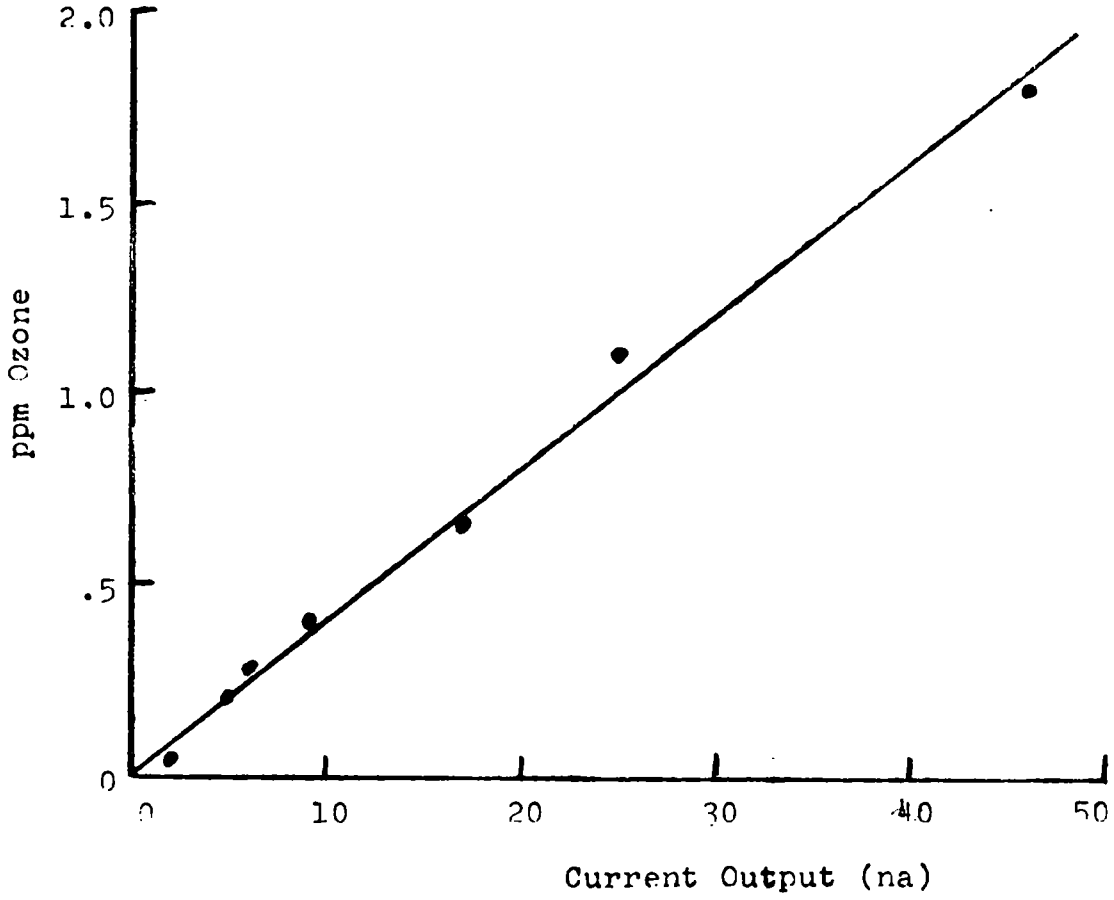

Figure 13 PMT Current vs. Meter Reading

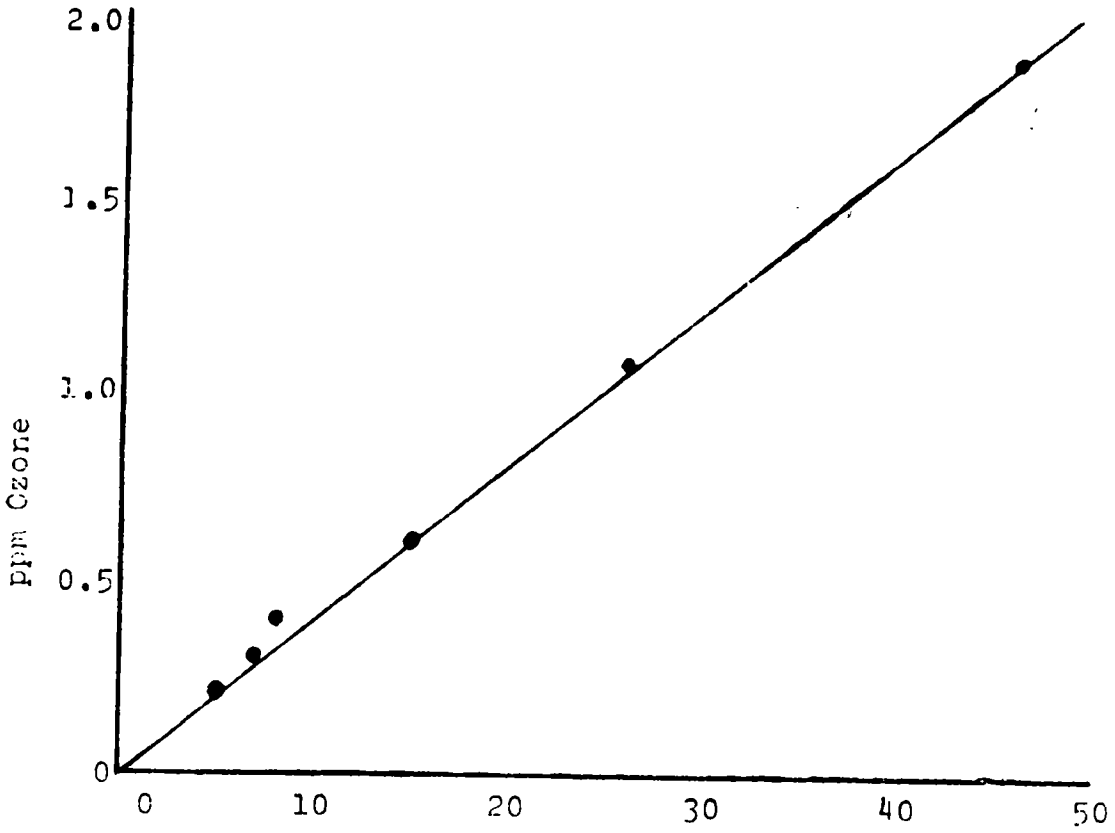

Figure 14 Ozone Concentration vs. LED Matrix Readout

when longer wavelength reactions such as NO_X - ozone are monitored.

As a further aid to thermionic noise reduction, some of the newer liquid crystal films such as N-(p-ethoxybenzylidene) -p-n-butylaniline should be tested as a chopper. This will function to alternately sense the background alone vs. the background plus signal without the complexity of mechanical choppers. This type of light chopper could be easily incorporated into photon counters simply by using up-down counters. The "on" cycles would count up, while the "off" cycles would count down. This then, would represent the ultimate in high reliability signal detection.

On the commercial aspects, the present transistor amplifier should definitely be replaced by an integrated system employing the new AM685 voltage comparator. This will provide faster response times, much greater reliability and stability, and a greater linear dynamic range. Also, the "brute-force" chain of decade dividers should be replaced by an integrated counter such as the Mostek MK5009P. This single chip device can divide by as much as 3.6×10^9, it's division is completely programmable, and it uses considerably less power than does a comparable number of TTL decade dividers.

The readout device can be any number of digital output devices. This includes numeral displays, printers, a computer, teletype lines, etc. In the device delivered, a 5 x 7 LED matrix was used with the idea that a permanent record could be made on photographic film. A more convenient readout would be a magnetic card such as used with the Hewlitt-Packard or Monroe desk-type computers. With this type of recording card, over a month's operation could be stored on one card. The card could then be entered into a computer to be collated with other

data. In any case, once the data is in digital form, many readout options are available.

APPENDIX A

Digital Division Circuitry

PAGE NOT

AVAILABLE

DIGITALLY

APPENDIX B

Photon Counter Description

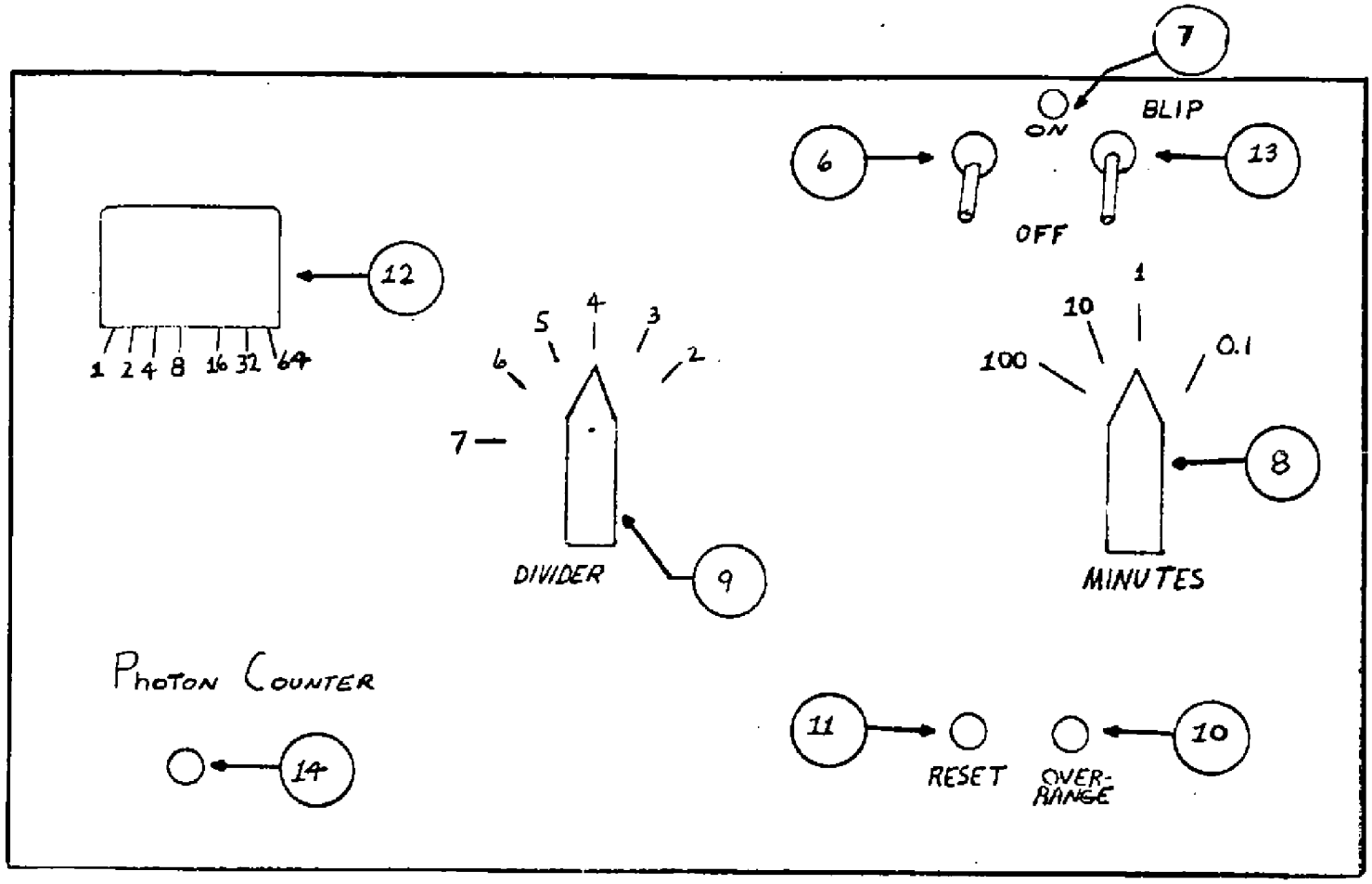
7
ON
BLIP
6
13
OFF
12
1 2 4 8 16 32 64
5
4
3
6
2
7
DIVIDER
9
1
10
100
0.1
8
MINUTES
Photon Counter
14
11
RESET
OVER-RANGE
10

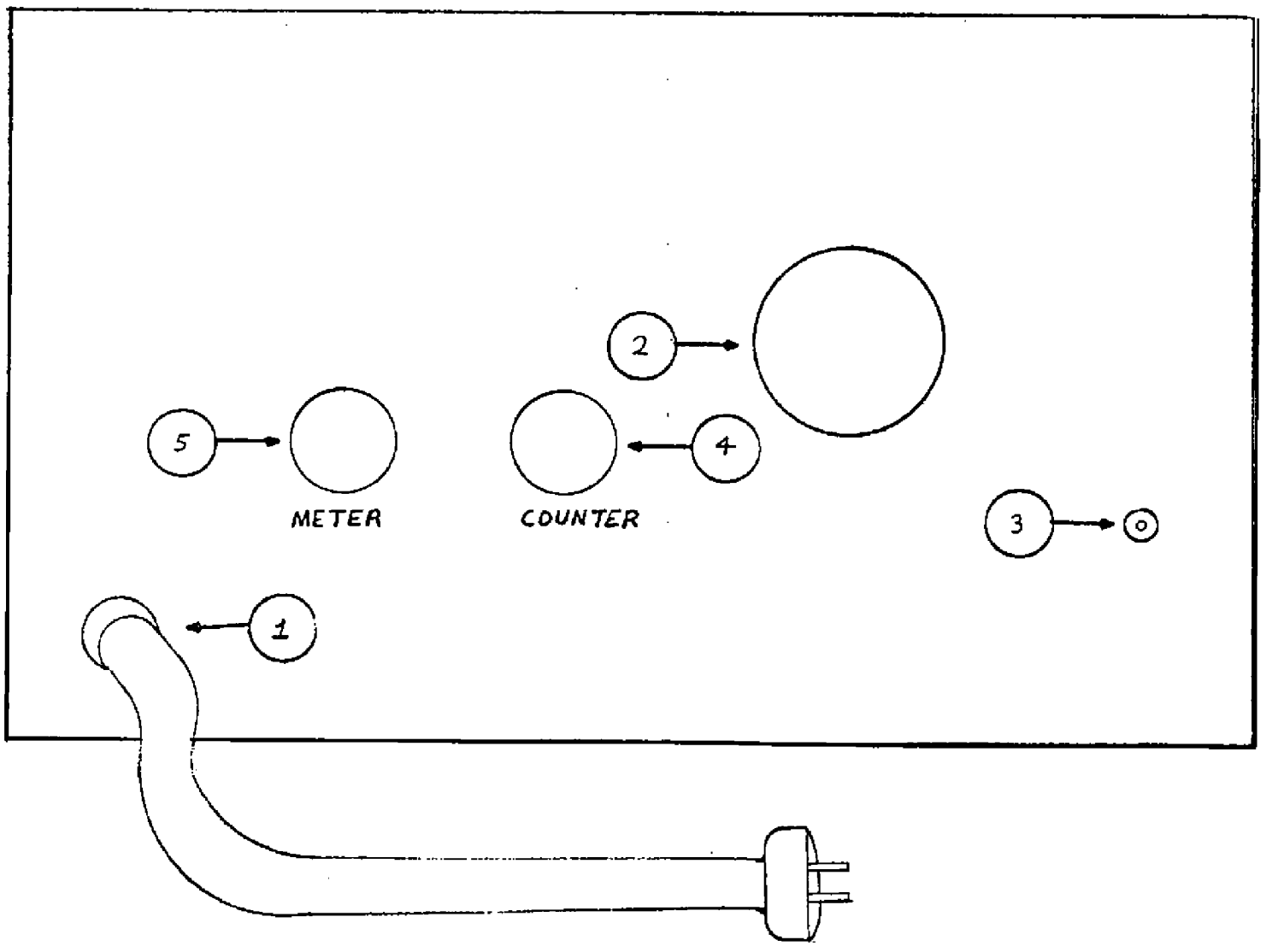
2
5
4
METER
COUNTER
3
1

APPENDIX B

Description of the Photon Counter

1. Electrical connector - 110v., 50-60 H_z.

2. Photomultiplier tube - mates directly with Meloy reaction chamber.

3. Preamp output - 0 - 0.1v. photoelectron signals prior to amplification.

4. Counter output - 0 5v. digital signals that can be connected to any digital counter.

5. Meter output - 0 - 10v., damped analog output. This signal corresponds to the conventional meter output used in most commercial chemiluminescence monitors.

6. On - off switch - this unit has essentially no warm-up time.

7. Indicator light - Operates from the main power supply to confirm that the unit is on.

8. Time adjust - sets the cycle rate to 0.1, 1, 10, or 100 minutes.

9. Divider - Divides the number of photon counts by exponent indicated (100 to 10 million). This should be set so that the LED readout (12) provides a reasonable reading.

10. Overrange indicator - Lights and stays on whenever the capacity of the LED readout (12) is exceeded (over 127 units).

11. Reset - This button should be pushed to turn the overrange indicator off.

12. LED readout - Contains 7 horizontal lamps and 5 vertical rows. The 7 horizontal lamps indicate a binary number between 1 and 127 which is proportional to ozone concentration. Each row normally indicates the accumulated photon counts for the previous cycle. After the current cycle time is completed, the lighted row will advance upward one row and display the latest reading.

13. Blip control - Inhibits the LED readout from constant indication. In the "Blip" position, the LED readout will display the accumulated counts for 0.1 second at the end of each cycle.

14. Threshold control - A screwdriver adjust potentiometer that permits the noise discrimination threshold to be increased or decreased.